**We would like to thank the referee for the thoughtful and insightful comments. We have addressed all of the comments. Our responses are itemized below.**

*The response appears sloppy. For example, the authors do not give the caption for the figure discussed in the 1st comment. In the 2nd comment, they add some references but not include references in the response. I have to go back to the revised manuscript to check what they are and whether the references are appropriate. Also, when they add some sentences in the revision, they do not give line numbers. Overall, the authors clarified most of my comments but there are still some unclear issues listed below. I recommend the minor revision of the paper before the possible acceptance of ACP by addressing my following comments.*

Thanks for the comments. We have now added the caption for the figure, references, and the line numbers in our responses.

*1) It is hard for me to understand your sentence filled with plus and minus sign in your response to my comments 11 and 13. Please try to interpret it using your own words and do not use math symbols.*

*Comments 11. On Page 11 Line 13, please describe the method you calculate horizontal mass fluxes at the four lateral boundaries in details. Clearly, the net effect does not equal to the fluxes summed with values from four lateral boundaries. How do you calculate the net effect of horizontal mass fluxes over the specific region?*

The horizontal mass fluxes and the net effects are summarized in Table 3. Revised to (P13L8-16) 'In northern China, the weakest (strongest) monsoon years in GEOS-4 show inflow fluxes of BC by 2.24 (0.97) kg $s^{-1}$ at the south boundary and by 6.60 (4.20) kg $s^{-1}$ at the west boundary, and outflow fluxes of BC by 3.44 (4.06) kg $s^{-1}$ at the north boundary and by 12.48 (9.20) kg $s^{-1}$ at the east boundary. The total effects are thus outflow fluxes by 7.08 kg $s^{-1}$ in the weakest monsoon years and by 8.09 kg $s^{-1}$ in the strongest monsoon years, resulting in a net effect of larger inflow of BC by 1.01 kg $s^{-1}$ in the weakest monsoon years than in the strongest monsoon years. Similarly, simulation results in MERRA show a net effect of larger inflow of BC by 1.60 kg $s^{-1}$ in the weakest monsoon years than in the strongest monsoon years.'

*Comments 13. On page 11 Lines 27-29, where do these two numbers (i.e., 0.09 and 0.27 kg/s) come from? Do you average them over the entire domain? Please specify the region your numbers are based on?*

Revised to (P23L8-30) 'In southern China, we find inflow fluxes of BC by 0.62 (0.70) kg $s^{-1}$ at the south boundary and by 0.94 (0.13) kg $s^{-1}$ at the west boundary, and outflow fluxes of BC by 1.79 (0.88) kg $s^{-1}$ at the north boundary and by 0.33 (0.42) kg $s^{-1}$ at the east boundary in the weakest (strongest) monsoon years in GEOS-4. The resulting effect is larger outflow fluxes of BC by 0.09 kg $s^{-1}$ in the weakest monsoon

years (0.56 kg $s^{-1}$) than in the strongest monsoon years (0.47 kg $s^{-1}$). In MERRA, the weakest monsoon years also show larger outflow fluxes of BC by 0.27 kg $s^{-1}$, compared to the strongest monsoon years.'

*2) It is too vague to me in their response to my comment 18 when the authors ascribed different BC concentration to different patterns of atmospheric circulation due to winter and summer monsoon. Please specify the cause the different response of BC to summer and winter monsoon (e.g., how these two types of monsoon system differently affects BC source, sink and transport in southern China?).*

*Comments 18. On Page 15, Lines 23-24, what is the cause of the different response of BC concentration to the summer and winter monsoon in southern china?*

Added discussions in (P20L15-22) 'The net effect in southern China is a larger inflow of BC by 0.19 (0.40) kg $s^{-1}$ in the weakest EAWM years than in the strongest EAWM years, which leads to the higher BC concentrations in the weakest EAWM years. As we discussed in Sect. 3.3, the larger outflow fluxes of BC by 0.09 (0.27) kg $s^{-1}$ result in the lower BC concentrations in southern China in the weakest EASM years than in the strongest EASM years. Different patterns of atmospheric circulation between summer and winter monsoon thus lead to the different distributions of BC in southern China. '

*3) I cannot find the authors' discussions in response to my comments 19 and 20 in the revised manuscript. Please give line numbers!*
*Comments 19. On Page 17, lines 21-24. I cannot tell the lower column burden of tropospheric BC from your Figure 5b. It appears that the BC profile increase at all altitudes. Is it related to the change of clouds?*

Added "Figs. 5(b right) and 10(b2)" in parentheses (P21L18). (P22L13-17) 'Relative to the strongest monsoon years, decreased BC concentrations are found in the weakest monsoon years …. from 1 to 6 km in the central China Plain. The decreased BC concentrations above 1–2 km lead to the reduction in the DRF in the two regions.'

*Comments 20. On Page 17, Lines 24-27, why is DRF lower in the weakest monsoon years in southern china even though both BC surface concentration and column burden are higher, compared with the strongest monsoon years?*

Added discussions (P21L22-23) 'We attribute these discrepancies largely to the vertical distributions of BC concentrations as discussed in the following paragraph.' (P22L13-17) 'Relative to the strongest monsoon years, decreased BC concentrations are found in the weakest monsoon years from 2 to 5 km in southern China …The decreased BC concentrations above 1–2 km lead to the reduction in the DRF in the two regions.'

**We would like to thank the referee for the thoughtful and insightful comments. We have addressed all of the comments. Our responses are itemized below.**

*This is a nicely written manuscript. This study is useful to understand the linkage of climate circulation and Asia pollution. I only have a few minor comments:*
*1) The spatial resolution used in this study is relatively coarse, and some potential uncertainties related to it may be discussed.*

Added discussions in Sect. 2.1 (P8L6-8) "We would like to point out that simulated BC concentrations are likely underestimated because of the …. and coarse resolution of the model used.".

*2) How much confidence do the authors have in simulating surface BC using GEOSChem? How about vertical profiles? The authors intensively investigated the impactof monsoon on vertical changes of BCs, but the first question is whether GEOS-Chemis able to capture the vertical profile of BC? How many uncertainties can be inferred from the potential bias of GEOS-Chem?*

Added discussions in Sect. 2.1 (P8L4-6) "We have systematically evaluated the BC simulations for 1980-2010 in China from the GEOS-Chem model (Li et al., 2016; Mao et al., 2016)." and in Sect. 3.4 (P15L7-12) "We would like to point out that few aircraft observations of BC vertical profile are available in China. Previous studies have evaluated the GEOS-Chem simulated vertical profiles of BC by using datasets from aircraft campaigns for the regions of the Northwest Pacific, North America, and the Arctic (Park et al., 2005; Drury et al., 2010; Wang et al., 2011).".

*3) In the abstract, Lines 17-18, whether the differences between the weakest EASM and strongest EASM years are significant. In another word, by looking at the entire simulation period, the authors can get the mean and the standard deviation of BC. How does this change magnitude (i.e., 0.04-0.09,0.03-0.04) compare to the 20-year variance? If we look at the inter-season variability (either summer or winter), do the weaker EASM always corresponds to higher BC whereas stronger EASM corresponds to lower BC?*

Thanks for the suggestions. Now mean and standard deviation of BC for 1986-2006 are included in Table 2 and the related discussions are in Sects. 3.3 (P11L22-25) and 4.3 (P20L5-8). "The difference in surface BC concentrations between the weakest and strongest summer monsoon years in each region is comparable or even larger than the corresponding standard deviation of JJA mean surface BC for 1986–2006 (Table 2).". "The difference in surface BC concentrations between the weakest and strongest winter monsoon years over each region is significant by comparing with the corresponding mean and standard deviation of DJF mean surface BC for 1986–2006

(Table 2).”

*4) Page 13, Line 22: the authors mentioned the effect due to non-China emissions. Maybe I missed something, I am not sure how the authors claim this impact is from non-China emissions.*

Added discussions in Sect. 2.1 (P7L29-P8L2) “We also conduct simulation (VNOC) to quantify the contributions of the non-China emissions to BC. The configurations of the model simulation are the same as those in VMET, except that anthropogenic and biomass burning emissions in China are set to zero.”

*5) Did the authors consider biogenic emissions in this study? If so, please add it. If not, please add the possible uncertainty due to this missing source.*

Added discussions in Sect. 2.1 (P7L12) “including both fossil fuel and biofuel emissions”.

*6) In the abstract (Line 14), the authors mentioned that the differences in BCs are mainly due to the circulation. I am wondering whether there are any way to quantify the effect from circulation change, wet deposition, etc.*

Thanks for the suggestion. Now the effect from circulation change and wet deposition are included in Table 3 and the role of wet deposition is discussed in Sects. 3.3 (P14L10-18) and 4.3 (P20L26-29). “We also examine the impact of the changes in precipitation associated with the strength of the summer monsoon on BC concentrations, which is not as dominant as that of the winds. Compared to the strongest EASM years, increases in wet deposition of BC are found in the weakest monsoon years north of 28 ° N in eastern China (Table 2), as a result of the high aerosol concentrations in the region and also the increased rainfall in the lower and middle reaches of the Yangtze River (around 30 ° N). In the region south of 28 ° N in eastern China, we find decreased wet deposition of BC in the weakest monsoon years because of the less rainfall and low BC concentrations in that region.” “Compared to the strongest EAWM years, enhanced wet deposition of BC are found in the weakest monsoon years in both northern and southern China (Table 2), likely because of the increased BC concentrations and precipitation in the corresponding regions.”

*7) The layouts of section 3 and 4 are interesting. These two parallel sections went through similar figures twice (one for summer and one for winter). Not sure whether this is the best way to discuss, but I think the figures showing summer and winter together look good.*

We would like to keep the Sect. 3 and 4 separately, which are likely readable and easy

to follow.

*8) Page 4, Line 17: L. Wang et al., 2014 Please remove "L."*

Deleted.

*9) Figure 3. Is the spatial correlation significant? One way is to use lines or markers to indicate statistical significance, or mask the areas insignificant.*

Thanks for the suggestion. The dotted areas added in Figure 3 indicate statistical significance with 95% confidence from a two-tailed Student's t-test.

References:

Drury, E., Jacob, D. J., Spurr, R. J. D., Wang, J., Shinozuka, Y., Anderson, B. E., Clarke, A. D., Dibb, J., McNaughton, C., and Weber, R.: Synthesis of satellite (MODIS), aircraft (ICARTT), and surface (IMPROVE, EPA-AQS, AERONET) aerosol observations over eastern North America to improve MODIS aerosol retrievals and constrain surface aerosol concentrations and sources, J. Geophys. Res. Atmos., 115 (D14), doi:10.1029/2009JD012629, 2010.

Park, R. J., Jacob, D. J., Palmer, P. I., Clarke, A. D., Weber, R. J., Zondlo, M. A., Eisele, F. L., Bandy, A. R., Thornton, D. C., Sachse, G. W., and Bond, T. C.: Export efficiency of black carbon aerosol in continental outflow: global implications, J. Geophys. Res. Atmos., 110 (D11), D11205, doi:10.1029/2004JD005432, 2005.

Wang, Q., Jacob, D. J., Fisher, J. A., Mao, J., Leibensperger, E. M., Carouge, C. C., Le Sager, P., Kondo, Y., Jimenez, J. L., Cubison, M. J., and Doherty, S. J.: Sources of carbonaceous aerosols and deposited black carbon in the Arctic in winter-spring: implications for radiative forcing, Atmos. Chem. Phys., 11(23), 12453–12473, doi:10.5194/acp-11-12453-2011, 2011.

**We would like to thank the referee for the thoughtful and insightful comments. We have addressed all of the comments. Our responses are itemized below.**

*In this work authors attempted to study the impacts of the interannual variation of Eastern Asian summer and winter monsoon on variations of black carbon (BC) mass concentrations and direct radiative forcing (DRF) in Eastern China during 1986-2006. Overall this paper is quite lengthy and reads more like a technical report. The results presented in the paper solely rely on model simulations lack of any observational evidences or cross-validation with previous modeling studies of BC. Some issues with respect to the method descriptions sound vague. The clarification of these issues is critical to understand comprehensive results presented in this study. I recommend the major revision of the paper before the possible acceptance of ACP by addressing my following comments.*

*Major comments:*
*1. The methodology used in this study simply followed previous studies [Zhu et al., 2012; Yang et al. 2014]. That's fine. The results of BC are not surprising to me at all since BC is one of important fine aerosol types (i.e., PM2.5) discussed in Zhu et al. [2012]. It might be more interesting to emphasize the change of special characteristics of BC (e.g., whether or how the change of cloud layer between weakest and strongest Eastern Asian monsoon impacts on the BC absorption and DRF).*

Thanks for the suggestion. We compare differences in JJA (DJF) cloud fraction (%) between the five weakest and five strongest EASM (EAWM) years during 1986–2006. Plots are averaged over longitude range of 110–125 °E based on MERRA. Compared to the five strongest EASM years, larger cloud fraction exists in northern China and also above ~7 km in southern China in the five weakest monsoon years. For winter monsoon, we find increased cloud fraction in southern China but decreased cloud below ~5 km in northern China in the weakest monsoon years. However, the impact of changes in cloud layer due to the monsoon on BC DRF is not as significant as that of changes in BC distributions due to the monsoon.

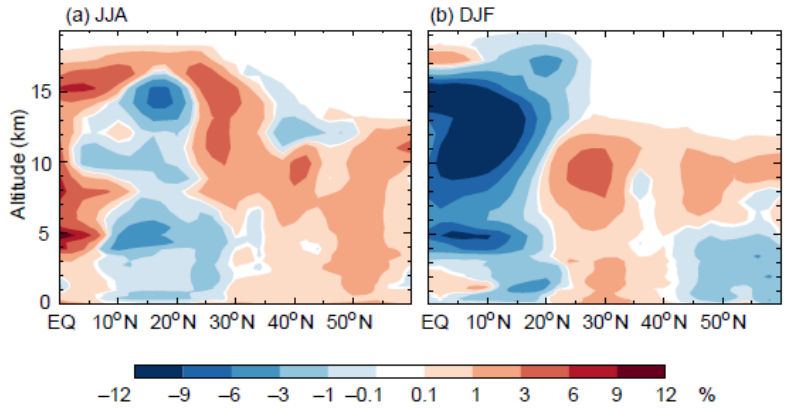


Fig. Differences in JJA (DJF) cloud fraction (%) between the five weakest and five strongest EASM (EAWM) years during 1986–2006.

Added discussions in Sect. 5 (P25L1-4) “It is also worth to point out that the BC DRF is also dependent on factors such as cloud and background aerosol distributions (Samset et al., 2011), which can be influenced by the strength of the EAM (Liu et al., 2010; Zhu et al., 2012)…These aspects should be further investigated in future studies”.

*2. The results presented in the paper solely rely on model simulations lack of any observational evidences or cross-validation with previous modeling studies of BC. This makes me wonder how the modeled BC mass concentrations in this work compare with historical observations available in Eastern China, especially during JJA and DJF (i.e., the seasons authors focus on in this work).*

Added discussions in Sect. 2.1 (P8L4-6) “We have systematically evaluated the BC simulations for 1980-2010 in China from the GEOS-Chem model (Li et al., 2016; Mao et al., 2016).

*3. Authors presented major results based on the difference between weakest and strongest Eastern Asia summer monsoon in Section 3 (covering Fig. 1a, Fig. 2a1, 2b1, Fig. 3a, . . .) and then from the difference in winter monsoon in Section 4 (covering Fig. 1b, Fig. 2a2,2b2, Fig. 3b, . . .). However, no discussions (linked to changes in winds or circulation patterns, etc) were made on the difference between summer and winter monsoon, which makes two sections sound like separate stories.*

Thanks for the suggestion. Added discussions in Sect. 5 (P24L27-28, P25L4-8)“Different patterns of atmospheric circulation between summer and winter monsoon lead to the different distributions of BC in southern and northern China.”…“In addition, the strength of the EAWM would influence the following summer monsoon via changes in the factors such as circulation and precipitation (e.g., Chen et al., 2000), and further affect the aerosols concentrations and radiative forcing. These aspects should be further investigated in future studies.”.

*4. Majority results in this work (i.e., Fig. 4-12, Table 2-5) highly reply on the difference between weakest and strongest Eastern Asia summer monsoon (in Section 3). The selection of five weakest and strongest years in this work is slightly different with previous studies [Zhu et al., 2012; Yang et al. 2014] that used the same GEOS-4 met fields of 1986-2006 without any explanations. Please explain why authors choose different monsoon years as adopted in Zhu et al. 2012 and Yang et al. 2014.*

Added discussions (P11L3-11) “we examine the differences in the JJA mean surface BC concentrations between five weakest (1988, 1993, 1995, 1996, and 1998) and five

strongest (1990, 1994, 1997, 2004, and 2006) EASM years during 1986–2006"… "We select these weakest (or strongest) monsoon years based on the five largest negative (or positive) values of the normalized EASMI in both GEOS-4 and MERRA within 1986–2006. The selected monsoon years are thus slightly different with those from previous studies (Zhu et al., 2012; Yang et al. 2014) only based on GEOS-4 (weakest monsoon years (1988, 1989, 1996, 1998, and 2003), and strongest monsoon years (1990, 1994, 1997, 2002, and 2006))."

*5. On Page 5 Line 26, should 1980-2010 be 1986-2006, which overlaps the period between GEOS-4 and MERRA?*

Revised as suggested (P6L5).

*6. On Page 8 Line 5-6, authors mentioned numerous studies have shown that the intensity of EAWM. . .. . .but they only cited one reference of Yan et al. (2009). It sounds contradictory.*

Added references "Guo et al., 1994; Ji et al., 1997; Chen et al., 2000; Jhun and Lee, 2004".

*7. In Section 3 and 4, authors enclosed values in the parenthesis but did not describe how they calculate these values, for instance the range of percentages on Page 8 Lines 22-23. Please add the clarification.*

Added clarification (P9L17)"the deviation from the mean (DM)".

*8. On Page 10 Lines 19-20, what is the cause of the different pattern of BC concentration between GEOS-4 and MERRA shown in Figure 5a?*

*Added discussion*s (P12L2-4) "The different patterns of BC concentrations between GEOS-4 and MERRA in Fig. 5a are likely because of the different convection schemes used in the two meteorological data (Rienecker et al., 2011)*."*

*9. On Page 11 Lines 2-3, how does the convergence cause the increase in BC concentration and anticyclone wind pattern cause the decrease in BC concentration?*

Added discussions (P12L9-14) "Relative to the strongest EASM years, anomalous northerlies over northern China and anomalous northeasterlies over the western North Pacific in the weakest EASM years prevent the outflow of pollutants from northern

China. In addition, southerly branch of the anomalous anticyclone in the south of the middle and lower reaches of the Yangtze River and nearby oceans strengthens the northward transport of aerosols from southern China to northern China.*"*.

*10. On Page 11, Lines 8-10, I understand the convergence accompanied with the descending air prevents surface BC to the upper troposphere, causing the increase in surface BC. But I don't understand why the upward mass flux of BC also increases under the condition of convergence. Could you explain it?*

Added discussions (P12L24-29) "Compared to the strong monsoon years, the increased surface BC concentrations in northern China lead to higher upward mass fluxes of BC concentrations north of 25 °N in both MERRA and GEOS-4. In southern China, the lower surface BC concentrations in the weakest EASM years result in the decreased upward fluxes south of 25 ° N. The pattern of the anomalous vertical transport of BC concentrations thus confirms the anomalous convergence in northern China and anomalous divergence in southern China in the weakest monsoon years.*"*

*11. On Page 11 Line 13, please describe the method you calculate horizontal mass fluxes at the four lateral boundaries in details. Clearly, the net effect does not equal to the fluxes summed with values from four lateral boundaries. How do you calculate the net effect of horizontal mass fluxes over the specific region?*

The horizontal mass fluxes and the net effects are summarized in Table 3. Revised to (P13L8-16) 'In northern China, the weakest (strongest) monsoon years in GEOS-4 show inflow fluxes of BC by 2.24 (0.97) kg $s^{-1}$ at the south boundary and by 6.60 (4.20) kg $s^{-1}$ at the west boundary, and outflow fluxes of BC by 3.44 (4.06) kg $s^{-1}$ at the north boundary and by 12.48 (9.20) kg $s^{-1}$ at the east boundary. The total effects are thus outflow fluxes by 7.08 kg $s^{-1}$ in the weakest monsoon years and by 8.09 kg $s^{-1}$ in the strongest monsoon years, resulting in a net effect of larger inflow of BC by 1.01 kg $s^{-1}$ in the weakest monsoon years than in the strongest monsoon years. Similarly, simulation results in MERRA show a net effect of larger inflow of BC by 1.60 kg $s^{-1}$ in the weakest monsoon years than in the strongest monsoon years.'

*12. On Page 11 Lines 23-25, why is there larger inflow at the east and north boundary and smaller outflow at the south and east boundary?*

Added discussions (P13L2-3) "The differences in winds between the weak and strong monsoon years lead to differences in horizontal transport of BC.*"*

*13. On page 11 Lines 27-29, where do these two numbers (i.e., 0.09 and 0.27 kg/s) come from? Do you average them over the entire domain? Please specify the region*

*your numbers are based on?*

Revised to (P23L8-30) 'In southern China, we find inflow fluxes of BC by 0.62 (0.70) kg $s^{-1}$ at the south boundary and by 0.94 (0.13) kg $s^{-1}$ at the west boundary, and outflow fluxes of BC by 1.79 (0.88) kg $s^{-1}$ at the north boundary and by 0.33 (0.42) kg $s^{-1}$ at the east boundary in the weakest (strongest) monsoon years in GEOS-4. The resulting effect is larger outflow fluxes of BC by 0.09 kg $s^{-1}$ in the weakest monsoon years (0.56 kg $s^{-1}$) than in the strongest monsoon years (0.47 kg $s^{-1}$). In MERRA, the weakest monsoon years also show larger outflow fluxes of BC by 0.27 kg $s^{-1}$, compared to the strongest monsoon years.'

*14. On Page 13, Lines 4-5, could you clarify what is the direct radiative forcing efficiency of BC? BTW, did you notice that the shift of the center of the highest BC DRF from weakest to strongest? Could you explain what is the cause of the shift?*

Added clarification in the parentheses in Sect. 3.4 (P14L2) "radiative forcing exerted per gram of BC". Added discussions (P16L4-8) "We find largest BC-induced forcing at the latitude of 30–40 ° N in the weakest monsoon years and 35–40 ° N in the strongest monsoon years. The shift of the center of the highest BC DRF is likely due to the different vertical distributions of BC concentrations between the weakest and strongest monsoon years (**Fig. 5a**)."

*15. On Page 13, Lines 18-21, please add quantitative metrics to quantify the change of BC DRF in northern and southern China.*

Added in Table 4.

*16. On Page 13, Lines 26-27, how do you distinguish the DRF of BC between non-China emission and local sources? Did you offline run the radiative transfer model? If yes, please describe it in the section of method.*

Added discussions in Sect. 2.1.(P7L29-P8L2) "We also conduct simulation (VNOC) to quantify the contributions of the non-China emissions to BC. The configurations of the model simulation are the same as those in VMET, except that anthropogenic and biomass burning emissions in China are set to zero.*"*

*17. On Page 14, line 22, could you show PBLH in the supplement? Also explain how PBLH changes surface BC concentration.*

Now included the PBLH in Figure S2. Also added discussions (P17L1-3) "The lower PBLH in MERRA suppresses the convection and thus leads to higher BC concentrations in the surface .".

*18. On Page 15, Lines 23-24, what is the cause of the different response of BC concentration to the summer and winter monsoon in southern china?*

Added discussions in (P20L15-22) 'The net effect in southern China is a larger inflow of BC by 0.19 (0.40) kg $s^{-1}$ in the weakest EAWM years than in the strongest EAWM years, which leads to the higher BC concentrations in the weakest EAWM years. As we discussed in Sect. 3.3, the larger outflow fluxes of BC by 0.09 (0.27) kg $s^{-1}$ result in the lower BC concentrations in southern China in the weakest EASM years than in the strongest EASM years. Different patterns of atmospheric circulation between summer and winter monsoon thus lead to the different distributions of BC in southern China. '

*19. On Page 17, lines 21-24. I cannot tell the lower column burden of tropospheric BC from your Figure 5b. It appears that the BC profile increase at all altitudes. Is it related to the change of clouds?*

Added "Figs. 5(b right) and 10(b2)" in parentheses (P21L18). (P22L13-17) 'Relative to the strongest monsoon years, decreased BC concentrations are found in the weakest monsoon years …. from 1 to 6 km in the central China Plain. The decreased BC concentrations above 1–2 km lead to the reduction in the DRF in the two regions.'

*20. On Page 17, Lines 24-27, why is DRF lower in the weakest monsoon years in southern china even though both BC surface concentration and column burden are higher, compared with the strongest monsoon years?*

Added discussions (P21L22-23) 'We attribute these discrepancies largely to the vertical distributions of BC concentrations as discussed in the following paragraph.' (P22L13-17) 'Relative to the strongest monsoon years, decreased BC concentrations are found in the weakest monsoon years from 2 to 5 km in southern China …The decreased BC concentrations above 1–2 km lead to the reduction in the DRF in the two regions.'

*21. On Page 20, besides simply reporting what you conclude in this work, could you add some discussion about why eastern Asian summer and winter monsoon change BC concentration and DRF in northern and southern China differently? Is this difference important to contribute to the air quality regulation in different regions of China?*

Added discussions in Sect. 5 (P24L29-P25L1) “Note that these different changes in BC concentrations and DRF between northern and southern China due to the EAM would be useful for proposing efficient air quality regulation in different regions of China.”

*22. On Page 5 Lines 17-18, BC is assumed externally mixed with other aerosol species in this model. Could authors discuss the uncertainties of your results based on this assumption? How do results change if BC is partially internally or internally mixed with other aerosol species?*

Thanks for the suggestion. Added discussions in Sect. 3.4 (P15L26-30) “Note that the estimated DRF is associated with large uncertainties due to the BC mixing state used in model, which assumes external mixing of aerosols and gives a lower-bound estimate of BC DRF. Internal mixing of BC with scattering aerosols in the real atmosphere likely increases the estimates of DRF (e.g., Jacobson, 2001).”.

*Minor comments:*

1. *Page 11 Line 12, change “summary” to “summarize”.*

   Revised.

2. *Figure 1, add the description of r31y and r21y.*

   Revised as “*r*_1980-2010” and “*r*_1986-2006”.

3. *Figure 4, please move the row of a2 above b1 since you discussed a2 ahead of b1 in the context.*

   Revised.

4. *Figure 10, please label a1, a2, b1, and b2 in Figure.*

   Revised.

5. *Figure 12, How do you distinguish BC concentration attributed to non-China emissions and local China sources in the model? Please specify in the description of the model.*

Added discussions in Sect. 2.1 (P7L29-P8L2): “We also conduct simulation (VNOC) to quantify the contributions of the non-China emissions to BC. The configurations of the model simulation are the same as those in VMET, except that anthropogenic and biomass burning emissions in China are set to zero.”.

**References:**


Chen, W., Graf, H., and Ronghui, H.: The interannual variability of East Asian Winter Monsoon and its relation to the summer monsoon, Adv. Atmos. Sci., 17, 48–60, doi:10.1007/s00376-000-0042-5, 2000.

Guo, Q.: Relationship between the variability of East Asia winter monsoon and temperature amomalies in China, Q. J. Appl. Meteorol., 5, 218-225, 1994 (in Chinese).

Jacobson, M. Z.: Strong radiative heating due to the mixing state of black carbon in atmospheric aerosols, Nature, 409, 695–697, 2001.

Ji, L., Sun, S., Arpe, K., and Bengtsson, L.: Model study on the interannual variability of Asian winter monsoon and its influence, Adv. Atmos. Sci., 14, 1-22, doi: 10.1007/s00376-997-0039-4, 1997.

Jhun, J.-G., and Lee, E.-J.: A New East Asian Winter Monsoon Index and Associated Characteristics of the Winter Monsoon, J. Clim., 17, 711–726, doi:10.1175/1520-0442(2004)017<0711:ANEAWM>2.0.CO;2, 2004.

**We would like to thank the referee for the thoughtful and insightful comments. We have addressed all of the comments. Our responses are itemized below.**

*This study used a chemistry transport model to examine the impact of monsoon variability on black carbon distribution (surface concentration, vertical profile and direct forcing as an integrated measure) over China. Since the emissions are fixed in the model simulation, metrological variability is the dominant sources of pollution variability. The results of this study generally support many empirical analyses that linked observed pollution level with monsoon variability as extensively cited in the paper. I found the analysis is comprehensive and the interpretation of the results is convincing. I recommend publication after the following issues are addressed.*

*One of my main concerns is regard to the interpretation of summer monsoon impact. It is noted by the authors " differences in transport of BC due to the changes in atmospheric circulation are a dominant mechanism through which the EASM influences the variations of JJA BC". However, the role of precipitation in setting wet removal is not adequately tested (e.g. excessive rainfall in strong monsoon year can increase wet removal flux and also contribute to pollution reduction). Of course, I admit that precipitation can also be correlated to circulation and moisture transport, so a deeper question would be. How do you separate the effects of circulation (dispersion) vs. rainfall (removal)?*

Points well taken. Now the differences in wet deposition are included in Table 3 and the role of wet deposition is discussed in Sects. 3.3 (P14L10-18) and 4.3 (P20L26-29). "We also examine the impact of the changes in precipitation associated with the strength of the summer monsoon on BC concentrations, which is not as dominant as that of the winds. Compared to the strongest EASM years, increases in wet deposition of BC are found in the weakest monsoon years north of 28 °N in eastern China (Table 2), as a result of the high aerosol concentrations in the region and also the increased rainfall in the lower and middle reaches of the Yangtze River (around 30 °N). In the region south of 28 °N in eastern China, we find decreased wet deposition of BC in the weakest monsoon years because of the less rainfall and low BC concentrations in that region. " "Compared to the strongest EAWM years, enhanced wet deposition of BC are found in the weakest monsoon years in both northern and southern China (Table 2), likely because of the increased BC concentrations and precipitation in the corresponding regions."

*For wintertime, it is reasonable that circulation is the main cause due to lack of rainfall generally. However, in explaining the higher surface concentrations in weaker monsoon years, how do you separate the effects of (1) weaker horizontal transport that leads to higher total column loading of pollution buildup and (2) weaker vertical mixing that tends to put more pollution at the surface? Are these two processes working in the same direction or now? Which is more important in the*

*model?*

Included discussions in Sect. 4.3 (P19L27-30, P20L29-P21L2) “Compared to the strongest monsoon years, increases in upward mass flux of BC concentrations are found over 20–30 °N and north of 40 °N in the troposphere in the weakest monsoon years, confirming the increased surface BC concentrations in northern and southern China (**Figs. 4b** and **5b**).” “Weaker upward transport in the weakest monsoon years than the strongest years above 1-2 km in southern China (Fig. **7b**) is also not a dominate factor that contributes to the higher surface BC concentrations in the region (Tables 2 and 3).”

*How do you account for the warming trends in the simulation years? Are the temperature/ precipitation trends significant? Are they leading to trends in pollutions?*

Added discussions in Sect. 3.3 (P14L19-24). “We would like to point out that warming trend is not a significant factor to the variations of BC concentrations in the present study, as emissions are fixed at the 2010 levels and warming trend in the emissions are thus excluded. In addition, Yang et al. (2016) have systematically examined the trends of metrological parameters and $PM_{2.5}$ in eastern China for 1985–2005. They found positive trend in temperature and negative trend in precipitation while no significant trends in BC concentrations.”.

*Minor points:*
*Page 1. Line 9. How do these affect "influence the variations of emissions"?*

*Added clarification in the* parentheses “biomass burning emissions*”.*

*Page 3. Line 19."convention" -> "convection"*

Revised.

*Page 2. Line 24. This is just repeating the reference in page 1?*

Deleted.

*Page 4. Line 7. "matters" -> "matter"*

Revised.

*Page 5. Line 5. What's a more appropriate reference here than Ramanathan and Carmichael (2008) is Ramanathan and Xu (2010).*

Revised.

*Line 11. It is odd to compare 1980-2010 forcing over Asia with 1850-2005 forcing globally.*

Deleted.

*Line 14. "Changes in monsoon"? But you did not provide references that monsoon was indeed changing over EA.*

References now included. Added (e.g., Menon et al., 2002; Lau et al., 2006)

*Line 22. If there is any statistical analysis on monsoon-BC relationship, they should be singled out and cited. Please check if any.*

Added discussions (P5L27-29) "Zhu et al. (2012) showed that simulated summer surface BC concentrations averaged over northern China (110–125 °E, 28–45 °N) are ~11% higher in the five weakest monsoon years than in the five strongest monsoon years for 1986–2006."

*Page 7. Line 6. What are the scaling factors in use? Previous analysis have shown BC emissions are biased low, and adjustment has be made to better agree with AAOD (Bond 2013) or radiative forcing (Xu et al., 2013) estimates from observations.*

Added discussions (P8L4-12) "We have systematically evaluated the BC simulations for 1980-2010 in China from the GEOS-Chem model (Li et al., 2016; Mao et al., 2016). We would like to point out that simulated BC concentrations are likely underestimated because of the biased low emissions (e.g., Bond et al., 2013; Xu et al., 2013; Mao et al., 2016) and coarse resolution of the model used. We discussed the adjustment of the biased low BC emissions using the scaling factor in our previous study by Mao et al. (2016). The adjustment of the BC emissions is not included in the present study, as we aim to discuss the impact of variations in meteorological parameters on BC. "

*Line 11. Do you have one run for each configuration? Or there is an ensemble of runs?*

Only one ensemble run for the configurations. Revised to "More details about the anthropogenic and biomass burning emissions of BC are discussed by Mao et al. (2016).".“In each simulation, meteorological parameters are allowed to vary year to year, but anthropogenic and biomass burning emissions of BC are fixed at the year 2010 levels.” (P7L19-21, 25-27).

*Page 8. Line 26. Could you comment on which is more reliable (if using NCEP as the benchmark)?*

Added discussions (P10L2-5) “MERRA is likely more reliable than the previous versions of GMAO metrological data products (e.g., GEOS-4 and GEOS-5), as MERRA has significant improved the convection and then precipitation and water vapor (Rienecker et al., 2011) by comparing to the reanalyses.”

*Page 16. Line 24. "summary" -> "summarize"*

Revised.

*Page 19. Since these two simulations are previously described in separated papers, it is worth noting if they are identical except for the meteorological field.*

The details about the configurations of the two simulations are now included in Sect. 2. (P7L25-27)

*Fig 8 and Fig 9. Statistical test of the difference should be conducted and reflected in the figure.*

The statistical analysis are included in Table 4 and the related Sects.3.4 and 4.4.

References:

Menon, S., Hansen, J., Nazarenko, L., and Luo, Y.: Climate effects of black carbon aerosols in China and India, Science, 297, 2250–2253, 2002.

Lau, K. M., M. K. Kim, and K. M. Kim, 2006: Asian summer monsoon anomalies induced by aerosol direct forcing: The role of the Tibetan Plateau, Climate Dyn., 26**,** 855–864.

Ramanathan, V., and Xu, Y. Y.: The Copenhagen Accord for limiting global warming:

Criteria, constraints, and available avenues, P. Natl. Acad. Sci. USA, 107(18), 8055–8062, doi:10.1073/pnas.1002293107, 2010.

# Impacts of East Asian Summer and Winter Monsoon on Interannual Variations of Mass Concentrations and Direct Radiative Forcing of Black Carbon over Eastern China

**Y. H. Mao[1*], H. Liao[1,2], and H. S. Chen[2,3,4]**

[1]School of Environmental Science and Engineering, Nanjing University of Information Science and Technology (NUIST), Nanjing 210044, China

[2]International Joint Research Laboratory on Climate and Environment Change (ILCEC), NUIST, Nanjing 210044, China

[3]Collaborative Innovation Center on Forecast and Evaluation of Meteorological Disasters (CIC)/Key Laboratory of Meteorological Disaster, Ministry of Education (KLME), NUIST, Nanjing 210044, China

[4]School of Atmospheric Sciences, NUIST, Nanjing 210044, China

带格式的：两端对齐

*Corresponding author address: Y. H. Mao (yhmao@nuist.edu.cn)

**Abstract.** We applied a global three-dimensional chemical transport model (GEOS-Chem) to examine the impacts of the East Asian monsoon on the interannual variations of mass concentrations and direct radiative forcing (DRF) of black carbon (BC) over eastern China (110–125 °E, 20–45 °N). With emissions fixed at the year 2010 levels, model simulations were driven by the Goddard Earth Observing System (GEOS-4) meteorological fields for 1986–2006 and the Modern Era Retrospective-analysis for Research and Applications (MERRA) meteorological fields for 1980–2010. During the period of 1986–2006, simulated JJA and DJF surface BC concentrations were higher in MERRA than in GEOS-4 by 0.30 μg $m^{-3}$ (44%) and 0.77 μg $m^{-3}$ (54%), respectively, because of the generally weaker precipitation in MERRA. We found that the strength of the East Asian summer monsoon (EASM, (East Asian winter monsoon, EAWM)) negatively correlated with simulated JJA (DJF) surface BC concentrations ($r$ = –0.7 (–0.7) in GEOS-4 and –0.4 (–0.7) in MERRA), mainly by the changes in atmospheric circulation. Relative to the five strongest EASM years, simulated JJA surface BC concentrations in the five weakest monsoon years were higher over northern China (110–125 °E, 28–45 °N) by 0.04–0.09 μg $m^{-3}$ (3–11%), but lower over southern China (110–125 °E, 20–27 °N) by 0.03–0.04 μg $m^{-3}$ (10–11%). Compared to the five strongest EAWM years, simulated DJF surface BC concentrations in the five weakest monsoon years were higher by 0.13–0.15 μg $m^{-3}$ (5–8%) in northern China and by 0.04–0.10 μg $m^{-3}$ (3–12%) in southern China. The resulting JJA (DJF) mean all-sky DRF of BC at the top of the atmosphere were 0.04 W $m^{-2}$ (3%, (0.03 W $m^{-2}$, 2%)) higher in northern China but 0.06 W $m^{-2}$ (14%, (0.03 W $m^{-2}$, 3%)) lower in southern China. In the weakest monsoon years, the weaker vertical convection at the elevated altitudes led to the lower BC concentrations above 1–2 km ~~above 1–2 km in southern China~~ in southern China, and therefore the lower BC DRF in the region. The differences in vertical profiles of BC between the weakest and strongest EASM years (1998–1997) and

EAWM years (1990–1996) reached up to –0.09 μg $m^{-3}$ (–46%) and –0.08 μg $m^{-3}$ (–11%) at 1–2 km in eastern China.

## 1 Introduction

High concentrations of aerosols in China have been reported in recent years (e.g., Zhang et al., 2008, 2012), which are largely attributed to the increases in emissions due to the rapid economic development. In addition, studies have shown that meteorological parameters are important factors in driving the interannual variations of aerosols in China (e.g., Jeong and Park, 2013; Mu and Liao, 2014; Yang et al., 2015). For example, Mu and Liao (2014) reported that meteorological parameters, e.g., precipitation, wind direction and wind speed, and boundary layer condition, significantly influence the variations of emissions (biomass burning emissions), transport, and deposition of aerosols.

China is located in the East Asian monsoon (EAM) domain. In a strong (weak) summer monsoon year, China experiences strong (weak) southerlies, large rainfall in northern (southern) China, and a deficit of rainfall in the middle and lower reaches of the Yangtze River (northern China) (Zhu et al., 2012). A strong winter monsoon is characterized by a stronger Siberian High and Aleutian Low (Chen et al., 2000), and China thus experiences stronger northerlies, more active cold surge, lower surface temperature, and excess snowfall (Jhun and Lee, 2004). The EAM has been reported to influence the interannual variations of aerosols in China, via in changes in monsoon circulation, precipitation, vertical convection, and etc. (e.g., Liu et al., 2010; Zhang et al., 2010a, 2010b; Yan et al., 2011; Zhu et al., 2012). The observed weakening EAM in recently years is also considered to contribute to the increase in aerosols in eastern Asia (e.g., Chang et al., 2000; Ding et al., 2008; Wang et al., 2009; Zhou et al., 2015).

Studies have reported that the strength of the East Asian summer monsoon (EASM) negatively influences the interannual variations of aerosols in eastern China.

Tan et al. (2015) showed that both the MODIS aerosol mass concentration and fine mode fraction in eastern China are high during weak monsoon years but low during active monsoon years for 2003–2013. By using the National Centers for Environmental Prediction/National Center for Atmospheric Research (NCEP/NCAR) reanalysis data and surface observations, Zhang et al. (2016) reported that the frequency of occurrence of cyclone related weather patterns decreases in the weak EASM years, which significantly degrades the air quality in northern China for 1980–2013. Modeling studies also reported that the strength of the EASM influences simulated aerosol concentrations and optical depths over eastern Asia (Zhang et al., 2010a, 2010b; Yan et al., 2011; Zhu et al., 2012). For example, Zhu et al. (2012) using a global chemical transport model (GEOS-Chem) found that simulated summer surface $PM_{2.5}$ (particulate matter~~s~~ with a diameter of 2.5 μm or less) concentrations averaged over eastern China (110–125 ° E, 20–45 ° N) are ~18% higher in the five weakest summer monsoon years than in the five strongest monsoon years for 1986–2006.

Similarly, negative correlations have been found between the strength of the East Asian winter monsoon (EAWM) and changes of air quality in eastern China. By analyzing the observed visibility and meteorological parameters from surface stations, studies have shown that the weak EAWM is related to the decrease of cold wave occurrence and surface wind speed, and therefore partially accounts for the decrease of winter visibility and the increase of number of haze days and the severe haze pollution events in China from 1960s (~~L.~~ Wang et al., 2014; Qu et al., 2015; Yin et al., 2015; Zhang et al., 2016). By further analyzing the reanalysis data, e.g., NCEP/NCAR and European Centre for Medium-Range Weather Forecasts (ECMWF), Li et al. (2015) showed that the stronger (weaker) EAWM is correlated with the less (more) wintertime fog–haze days. The weak EAWM results in a reduction of wind speed and decline in the frequency of northerly winds, which leads to an increase in the number of haze days and occurrences of severe haze events (Chen and Wang, 2015; Zhou et al., 2015). ~~Zhang et al. (2016) reported that the strong EAWM increases the frequency of occurrence of anticyclone-related weather patterns and therefore improves the air~~

~~quality in northern China for 1980–2013.~~

Black carbon (BC) as a chemically inert species is a good tracer to investigate the impact of the meteorological parameters and the EAM on the interannual variations of aerosols. BC is an important short-lived aerosol; the reduction of BC emissions is identified as a near-term approach to benefit the human health, air quality, and climate change efficiently (Ramanathan and Xu, 2010~~Ramanathan and Carmichael, 2008~~; Shindell et al., 2012; Bond et al., 2013; IPCC, 2013; Smith et al., 2013). BC emissions in China have been dramatically increased in the recent several decades, which contribute about 25% of the global total emissions (Cooke et al., 1999; Bond et al., 2004; Lu et al., 2011; Qin and Xie, 2012; Wang et al., 2012). Observed annual mean surface BC concentrations are typically about 2–5 μg $m^{-3}$ at rural sites (Zhang et al., 2008). Simulated annual direct radiative forcing (DRF) due to BC at the top of the atmosphere (TOA) is in the range of 0.58–1.46 W $m^{-2}$ in China, reported by previous modeling studies (summarized in Li et al., 2016). Mao et al. (2016) using the GEOS-Chem model showed that annual mean BC DRF averaged over China increases by 0.35 W $m^{-2}$ (51%) between 2010 and 1980~~, which is comparable to the global annual mean DRF values of BC (0.4 W $m^{-2}$), tropospheric ozone (0.4 W $m^{-2}$), and carbon dioxide (1.82 W $m^{-2}$) (IPCC, 2013)~~.

带格式的：字体：倾斜

The changes in BC concentrations in China are coupled with the changes in monsoon (e.g., Menon et al., 2002; Lau et al., 2006). Studies in the past decades were generally focused on the impacts of BC on the Asian monsoon (Menon et al., 2002; Lau et al., 2006; Meehl et al., 2007; Bollasina et al., 2011). Studies also showed that the climate effect of increasing BC could partially explain the "north drought/south flooding" precipitation pattern in China in recent decades (e.g., Menon et al., 2002; Gu et al., 2010). Conversely, the EAM could influence the spatial and vertical distributions of BC concentrations and further the radiative forcing and climate effect of BC. Zhu et al. (2012) showed that simulated summer surface BC concentrations averaged over northern China (110–125 ° E, 28–45 ° N) are ~11% higher in the five weakest monsoon years than in the five strongest monsoon years for 1986–2006. However, to our knowledge, few studies have systematically quantified the impact the

EAM (especially the EAWM) on the variations of concentrations and DRF of BC in China.

The goal of the present study is to improve our understanding of the impacts of the EAM on the interannual variations of surface concentrations, vertical distributions, and DRF of BC in eastern China for 19860–20060. We aim to examine the mechanisms through which the EASM and EAWM influence the variations of BC. We describe the GEOS-Chem model and numerical simulations in Sect. 2. Sect. 3 shows simulated impacts of the EASM on interannual variations of June-July-August (JJA) BC in eastern China and examines the influence mechanisms. Sect. 4 presents the impacts of the EAWM on interannual variations of December-January-February (DJF) BC and the relevant mechanisms. Summary and conclusions are given in Sect. 5.

## 2 Methods

### 2.1 GEOS-Chem Model and Numerical Experiments

The GEOS-Chem model is driven by assimilated meteorology from the Goddard Earth Observing System (GEOS) of the NASA Global Modeling and Assimilation Office (GMAO, Bey et al., 2001). Here we use GEOS-Chem version 9-01-03 (available at http://geos-chem.org) driven by the GEOS-4 and the Modern Era Retrospective-analysis for Research and Applications (MERRA) meteorological fields (Rienecker et al., 2011), with 6 h temporal resolution (3 h for surface variables and mixing depths), 2 ° (latitude) × 2.5 ° (longitude) horizontal resolution, and 30 (GEOS-4) or 47 (MERRA) vertical layers from the surface to 0.01 hPa. The GEOS-Chem simulation of carbonaceous aerosols has been reported previously by Park et al. (2003). Eighty percent of BC emitted from primary sources is assumed to be hydrophobic, and hydrophobic aerosols become hydrophilic with an e-folding time of 1.2 days (Cooke et al., 1999; Chin et al., 2002; Park et al., 2003). BC in the model is assumed to be externally mixed with other aerosol species.

Tracer advection is computed every 15 minutes with a flux-form semi-Lagrangian

method (Lin and Rood, 1996). Tracer moist convection is computed using GEOS convective, entrainment, and detrainment mass fluxes as described by Allen et al. (1996a, b). The deep convection scheme of GEOS-4 is based on Zhang and McFarlane (1995), and the shallow convection treatment follows Hack (1994). MERRA convection is parameterized using the relaxed Arakawa-Schubert scheme (Arakawa and Schubert, 1974; Moorthi and Suarez, 1992). Simulation of aerosol wet and dry deposition follows Liu et al. (2001) and is updated by Wang et al. (2011). Wet deposition includes contributions from scavenging in convective updrafts, rainout from convective anvils, and rainout and washout from large-scale precipitation. Dry deposition of aerosols uses a resistance-in-series model (Walcek et al., 1986) dependent on local surface type and meteorological conditions.

The anthropogenic emissions of BC, including both fossil fuel and biofuel emissions, are from Bond et al. (2007) globally and updated in Asia (60 ° E–150 ° E, 10 ° S–55 ° N) with the Regional Emission inventory in Asia (REAS, available at http://www.jamstec.go.jp/frsgc/research/d4/emission.htm, Ohara et al., 2007). Seasonal variations of anthropogenic emissions are considered in China and Indian using monthly scaling factors taken from Kurokawa et al. (2013). Global biomass burning emissions of BC are taken from the Global Fire Emissions Database version 3 (GFEDv3, van der Werf et al., 2010) with a monthly temporal resolution. More details about the ~~configuration~~ anthropogenic and biomass burning emissions of BC ~~emissions~~ are discussed by Mao et al. (2016).

We conduct two simulations driven by GEOS-4 for years 1986–2006 (VMETG4) and by MERRA for 1980–2010 (VMET). Our analysis centers on the period of 1986–2006, the years for which both GEOS-4 and MERRA data are available. Both simulations are preceded by 1-year spin up. In ~~the~~ each simulation~~s~~, meteorological parameters are allowed to vary year to year, but anthropogenic and biomass burning emissions of BC are fixed at the year 2010 levels. The simulations thus represent the impact of variations in meteorological parameters on the interannual variations of BC. We also conduct simulation (VNOC) to quantify the contributions of the non-China emissions to BC. The configurations of the model simulation are the same as those in

VMET, except that anthropogenic and biomass burning emissions in China are set to zero. The evaluations of GEOS-Chem aerosol simulations in China using the MERRA and GEOS-4 data are discussed in the studies, e.g., Mao et al. (2016) and Yang et al. (2015), respectively. In addition, we have systematically evaluated the BC simulations for 1980-2010 in China from the GEOS-Chem model (Li et al., 2016; Mao et al., 2016). We would like to point out that simulated BC concentrations are likely underestimated because of the biased low emissions (e.g., Bond et al., 2013; Xu et al., 2013; Mao et al., 2016) and coarse resolution of the model used. We have discussed the adjustment of the biased low BC emissions using the scaling factor in our previous study by Mao et al. (2016). The adjustment of the BC emissions is not included in the present study, as we aim to discuss the impact of variations in meteorological parameters on BC.

带格式的：缩进：首行缩进： 0 字符

## 2.2 The Definition of EAM Index

The interannual variations in the strength of the EAM are commonly represented by the indexes. Following Zhu et al. (2012) and Yang et al. (2014), we use the EASM index (EASMI, **Fig. 1a**) introduced by Li and Zeng (2002) in the present study based on the GEOS-4 meteorological parameters for 1986–2006 or the MERRA data for 1980–2010 (referred to as EASMI_GEOS and EASMI_MERRA, respectively). The EASMI calculated using the reanalyzed NCEP/NCAR datasets (Kalnay et al., 1996; Zhu et al., 2012, referred to as EASMI_NCEP, not shown) agrees well ($r > 0.97$) with EASMI_GEOS for 1986–2006 and with EASMI_MERRA for 1980–2010, indicating that both the GEOS-4 and MERRA data have a good representation of the strength of the EASM. Positive values of EASMI indicate strong summer monsoon years while negative values indicate weak monsoon years.

Numerous studies have shown that the intensity of the EAWM is closely tied with wind, air temperature, and precipitation (e.g., Guo et al., 1994; Ji et al., 1997; Chen et al., 2000; Jhun and Lee, 2004; Yan et al., 2009). The definitions of the EAWM index

(EAWMI) are thus quite different in the previous studies (Table 1). Here we calculate the EAWMI (**Fig. 1b**) as the sum of zonal sea level pressure differences (110 ° E vs.160 ° E) over 20–70 ° N, following Wu and Wang (2002). The EAWMIs in GEOS-4 and MERRA (referred to as EAWMI_GEOS and EAWMI_MERRA) in the present study show strong correlations with those based on surface temperature, wind, and pressure ($r$ = 0.51–0.82, Table 1) and are generally consistent with that in NECP (referred to as EAWMI_NCEP), with the correlation coefficients larger than 0.94. The EAWMIs in GEOS and MERRA are thus reliable to represent the strength of the EAWM. Similarly, negative (positive) values of EAWMI indicate weak (strong) winter monsoon years.

## 3. Impact of EASM on Interannual Variation of BC

### 3.1 Simulated JJA BC in GEOS-4 and MERRA

**Fig. 1a** also show simulated JJA surface concentrations of BC averaged over eastern China (110–125 ° E, 20–45 ° N). Simulated JJA surface concentrations of BC have strong interannual variations, which range from 0.95–1.04 μg $m^{-3}$ with ~~(~~the deviation from the mean (DM) of –5.3% to 4.2%~~)~~ in VMET and 0.65–0.78 μg $m^{-3}$ with the DM of ~~(~~–6.8% to 12.5%~~)~~ in VMETG4. During the period of 1986–2006, JJA surface BC concentrations on average are 0.30 μg $m^{-3}$ (44%) higher in MERRA than in GEOS-4. Our analyses indicate that different precipitation patterns between GEOS-4 and MERRA likely account for the abovementioned differences in BC concentrations using the two meteorological fields.

We find that the JJA mean precipitation is stronger in GEOS-4 than in MERRA in most of China, except in southern China (**Fig. 1S**). In **Fig. 2a**, we further compare the differences in precipitation between GEOS-4 and MERRA averaged over eastern China. The JJA mean precipitation in GEOS-4 is 2.5 mm $d^{-1}$ (29%) stronger than that in MERRA for 1986–2006. The resulting wet deposition (**Fig. 2b**) is also higher by 0.018 kg $s^{-1}$ (11%) in GEOS-4 than in MERRA. The stronger precipitation in

GEOS-4 thus results in the significantly lower surface BC concentrations. Note that MERRA is likely more reliable than the previous versions of GMAO metrological data products (e.g., GEOS-4 and GEOS-5), as MERRA has significant improved the convection and then precipitation and water vapor by comparing to the reanalyses (Rienecker et al., 2011). ~~The stronger precipitation in GEOS-4 thus results in the significantly lower surface BC concentrations.~~

带格式的: 字体: (默认) Times New Roman, 小四

带格式的: 字体: (默认) Times New Roman, 小四

带格式的: 字体: (中文) +中文正文 (宋体)

### 3.2 Correlation between JJA BC and EASMI

In simulations VMET and VMETG4, we find that monsoon strength has large impacts on summertime BC concentrations over eastern China. JJA surface concentrations of BC negatively correlate with both the EASMI_GEOS4 and EASMI_MERRA (**Fig. 1a**). The correlation coefficient between simulated surface BC concentrations and the EASMI_GEOS4 is –0.7 for 1986–2006, and those for the EASMI_MERRA are –0.5 for 1980–2010 and –0.4 for 1986–2006. Simulated surface BC concentrations are thus high (low) in the weak (strong) EASM years.

**Fig. 3a** shows the spatial distributions of the correlation coefficients between BC surface concentrations and the EASMI_GEOS4 or EASMI_MERRA. Negative correlations are found in central and northeastern China with the strongest negative correlations in eastern China and the Tibetan Plateau (<–0.8), while positive correlations are over southern and northwestern China with the largest values in southern China (> 0.7). The correlation coefficients in GEOS-4 and MERRA show similar spatial distribution and magnitude, except that positive correlations are found in larger regions in MERRA than in GEOS-4. Our results are generally consistent with those from Zhu et al. (2012), which reported that surface concentrations of $PM_{2.5}$ in GEOS-4 are high in northern China (110–125 °E, 28–45 °N) but low in southern China (110–125 °E, 20–27 °N) in the weak EASM years than in the strong monsoon years.

### 3.3 Differences in BC between Weak and Strong EASM years

In order to quantify to what degree the strength of the EASM influences surface BC concentrations in China, we examine the differences in the JJA mean surface BC concentrations between five weakest (1988, 1993, 1995, 1996, and 1998) and five strongest (1990, 1994, 1997, 2004, and 2006) EASM years during 1986–2006 (**Fig. 4a**). We select these weakest (or strongest) monsoon years based on the five largest negative (or positive) values of the normalized EASMI in both GEOS-4 and MERRA within 1986–2006. The selected monsoon years are thus slightly different with those from previous studies (Zhu et al., 2012; Yang et al. 2014) only based on GEOS-4 (weakest monsoon years (1988, 1989, 1996, 1998, and 2003), and strongest monsoon years (1990, 1994, 1997, 2002, and 2006)). The spatial distribution of the differences in concentrations between the weakest and strongest summer monsoon years is in good agreement with the distribution of the correlation coefficients between concentrations and EASMI (**Fig. 3a**). The differences in JJA mean surface BC concentrations are highest in northern China with a maximum exceeding 0.3 μg $m^{-3}$ (40%). Relative to the strongest summer monsoon years, JJA surface BC concentrations in GEOS-4 in the weakest summer monsoon years are 0.09 μg $m^{-3}$ (11%) higher over northern China and 0.03 μg $m^{-3}$ (11%) lower over southern China (Table 2). The corresponding values in MERRA are 0.04 μg $m^{-3}$ (3%) higher over northern China and 0.04 μg $m^{-3}$ (10%) lower over southern China. In the eastern China, JJA surface BC concentrations in the weakest monsoon years are higher on average by 0.05 μg $m^{-3}$ (9%) in GEOS-4 and by 0.02 μg $m^{-3}$ (2%) in MERRA. The difference in surface BC concentrations between the weakest and strongest summer monsoon years in each region is comparable or even larger than the corresponding standard deviation of JJA mean surface BC for 1986–2006 (Table 2). The different patterns of BC concentrations between northern and southern China can also been see in **Fig. 5a**, which shows the height-latitude plot of the differences in BC concentrations averaged over 110–125 °E between the five weakest and five strongest monsoon years. BC concentrations in the whole troposphere are lower south of 27 °N

带格式的：字体：非倾斜
带格式的：字体：非倾斜
带格式的：字体：非倾斜
带格式的：字体：非倾斜

but higher north of 27 °N in the weakest monsoon years than in the strongest years. The different patterns of BC concentrations between GEOS-4 and MERRA in Fig. 5a are likely because of the different convection schemes used in the two meteorological data (Rienecker et al., 2011).

Zhu et al. (2012) have shown that the impacts of the EASM on aerosol concentrations in eastern China are mainly by the changes in atmospheric circulation. **Fig. 6a** shows composite differences in JJA 850 hPa wind (m $s^{-1}$) between the five weakest and five strongest EASM years from the GEOS-4 and MERRA data. ~~Relative to the strong EASM years~~ Relative to the strongest EASM years, anomalous northerlies over northern China and anomalous northeasterlies over the western North Pacific in the weakest monsoon years prevent the outflow of pollutants from northern China. In addition, southerly branch of the anomalous anticyclone in the south of the middle and lower reaches of the Yangtze River and nearby oceans strengthens the northward transport of aerosols from southern China to northern China. As a result, an anomalous convergence in northern China leads to an increase in BC concentrations in the region, while an anomalous anticyclone in the south of the middle and lower reaches of the Yangtze River results in the decreased BC concentrations in southern China ~~, an anomalous convergence in northern China leads to an increase in BC concentrations in the weak EASM years in the region, while an anomalous anticyclone in the south of the middle and lower reaches of the Yangtze River and nearby oceans results in the decreased BC concentrations in southern China~~ (**Fig. 4a**). The convergence and divergence can also be seen in **Fig. 7a**, which shows anomalous ~~vertical transport~~vertical transport of BC concentrations averaged over 110–125 °E. Compared to the strong monsoon years, the increased surface BC concentrations in northern China lead to higher upward mass fluxes of BC concentrations ~~are found~~ north of 25 °N in both MERRA and GEOS-4 ~~in both MERRA and GEOS-4,~~. In southern China, ~~while~~ the lower surface BC concentrations in the weakest EASM years result in the decreased upward fluxes ~~exist~~ south of 25 °N. The pattern of the anomalous vertical transport of BC concentrations thus confirms the anomalous convergence in northern China and anomalous divergence in southern China in the

weakest monsoon years.

The differences in winds between the weak and strong monsoon years lead to differences in horizontal transport of BC. We summarizey in Table 3 the differences in simulated horizontal mass fluxes of JJA BC at the four lateral boundaries of the box in northern and southern China (**Fig. 4a**, from the surface to 10 km), based on simulations VMETG4 and VMET. The boxes are selected as BC concentrations in the regions are higher or lower in the weakest monsoon years than in the strongest monsoon years (**Fig. 4a**). In northern China, the weakest (strongest) monsoon years in GEOS-4 show inflow fluxes of BC by 2.24 (0.97) kg $s^{-1}$ at the south boundary and by 6.60 (4.20) kg $s^{-1}$ –at the west boundary, and outflow fluxes of BC by 3.44 (4.06) kg $s^{-1}$ at the north boundary and by 12.48 (9.20) kg $s^{-1}$ at the east boundary. The total effects are thus outflow fluxes by 7.08 kg $s^{-1}$ in the weakest monsoon years and by 8.09 kg $s^{-1}$ in the strongest monsoon years, resulting in a net effect of larger inflow of BC by 1.01 kg $s^{-1}$ in the weakest monsoon years than in the strongest monsoon years. Similarly, simulation results in MERRA show a net effect of larger inflow of BC by 1.60 kg $s^{-1}$ in the weakest monsoon years than in the strongest monsoon years. ~~larger inflow fluxes of BC by 1.27 (1.01) and 2.40 (1.21) kg $s^{-1}$, respectively, at the south and west boundaries, lower outflow by 0.62 (0.67) kg $s^{-1}$ at the north boundary, and larger outflow by 3.28 (1.29) kg $s^{-1}$ at the east boundary, based on simulation VMETG4 (VMET). The net effect is a larger inflow of BC by 1.01 (1.60) kg $s^{-1}$,~~The larger inflow of BC in the weakest monsoon years ~~which~~thus –leads to the higher surface BC concentrations in northern ~~the weakest monsoon years in northern~~ China. In southern China, we find inflow fluxes of BC by 0.62 (0.70) kg $s^{-1}$ at the south boundary and by 0.94 (0.13) kg $s^{-1}$ at the west boundary, and outflow fluxes of BC by 1.79 (0.88) kg $s^{-1}$ at the north boundary and by 0.33 (0.42) kg $s^{-1}$ at the east boundary in the weakest (strongest) monsoon years in GEOS-4. The resulting effect is larger outflow fluxes of BC by 0.09 kg $s^{-1}$ in the weakest monsoon years (0.56 kg $s^{-1}$) than in the strongest monsoon years (0.47 kg $s^{-1}$). In MERRA, the weakest monsoon years also show larger outflow fluxes of BC by 0.27 kg $s^{-1}$, compared to the strongest monsoon years. ~~larger inflow by 0.81 (0.35) kg $s^{-1}$ at the west boundary, larger~~

带格式的：缩进：首行缩进： 2 字符，定义网格后自动调整右缩进，段落间距段后：10 磅，孤行控制，调整中文与西文文字的间距，调整中文与数字的间距

~~outflow by 0.91 (0.72) kg s$^{-1}$ at the north boundary, and less outflow by 0.09 (0.09) kg s$^{-1}$ at the east boundary. Relative to the strongest monsoon years, the inflow in the south boundary in the weakest monsoon years is less by 0.09 kg s$^{-1}$ in GEOS-4 and larger by 0.01 kg s$^{-1}$ in MERRA. As a result, the weakest monsoon years have larger outflow fluxes of 0.09 and 0.27 kg s$^{-1}$ than the strongest monsoon years in GEOS-4 and in MERRA, respectively.~~ These results indicate that the differences in transport of BC due to the changes in atmospheric circulation are a dominant mechanism through which the EASM influences the variations of JJA BC concentrations in eastern China.

We also examine the impact of the changes in precipitation associated with the strength of the summer monsoon on BC concentrations, which is not as dominant as that of the winds. Compared to the strongest EASM years, increases in wet deposition of BC are found in the weakest monsoon years north of 28 °N in eastern China (Table 2), as a result of the high aerosol concentrations in the region and also the increased rainfall in the lower and middle reaches of the Yangtze River (around 30 °N). In the region south of 28 °N in eastern China, we find decreased wet deposition of BC in the weakest monsoon years because of the less rainfall and low BC concentrations in that region.

We would like to point out that warming trend is not a significant factor to the variations of BC concentrations in the present study, as emissions are fixed at the 2010 levels and warming trend in the emissions is thus excluded. In addition, Yang et al. (2016) have systematically examined the trends of metrological parameters and $PM_{2.5}$ in eastern China for 1985–2005. They found positive trend in temperature and negative trend in precipitation while no significant trend in BC concentrations.

–

### 3.4 Impact of EASM on Vertical Profile and DRF of BC

Previous studies have shown that vertical distribution of BC is critical for the calculation of the BC DRF (e.g., Bond et al., 2013; Li et al., 2016). The calculation of

带格式的：首行缩进： 2 字符

带格式的：缩进：首行缩进： 1.18 字符

the BC DRF is dependent on several factors, e.g., BC lifetime and radiative forcing efficiency (radiative forcing exerted per gram of BC), which are significantly influenced by vertical distribution of BC. Vertical profile of BC affects its wet scavenging and hence its lifetime (Bond et al., 2013). The direct radiative forcing efficiency of BC enhanced considerably when BC is located at high altitude largely because of the radiative interactions with clouds (Samset et al., 2013). For example, BC above 5 km accounts for ~40% of the global DRF of BC (Samset et al., 2013). We would like to point out that few aircraft observations of BC vertical profile are available in China. Previous studies have evaluated the GEOS-Chem simulated vertical profiles of BC by using datasets from aircraft campaigns for the regions of the Northwest Pacific, North America, and the Arctic (Park et al., 2005; Drury et al., 2010; Wang et al., 2011).

**Fig. 8a** compares the simulated JJA mean all-sky DRF of BC at the TOA in the five weakest and five strongest EASM years during 1986–2006. Model results are from simulation VMET. The BC DRF is calculated using the Rapid Radiative Transfer Model for GCMs (RRTMG, Heald et al., 2014), which is discussed in details by Mao et al. (2016). We find that the BC DRF is highest (> 3.0 W $m^{-2}$) over northern China in JJA. The spatial distributions of the differences in the BC DRF between the weakest and strongest monsoon years are similar to those in BC concentrations (**Fig. 4a**). Relative to the strongest monsoon years, the TOA DRF of BC shows an increase north of 28 °N while a reduction south of 27 °N in the weakest monsoon years. The BC DRF in northern China is 0.04 W $m^{-2}$ (3%, Table 4) higher in the weakest than strongest monsoon years, with a maximum of 0.3 W $m^{-2}$ in Jiangsu province. In southern China, the weakest monsoon years have a lower DRF by 0.06 W $m^{-2}$ (14%). As a result, the TOA DRF of BC in eastern China is 0.01 W $m^{-2}$ (1%) higher in the weakest monsoon years than in the strongest monsoon years. Note that the estimated DRF is associated with large uncertainties due to the BC mixing state used in model, which assumes external mixing of aerosols and gives a lower-bound estimate of BC DRF. Internal mixing of BC with scattering aerosols in the real atmosphere likely increases the estimates of DRF (e.g., Jacobson, 2001).

We further compare in **Fig. 9a** the vertical distribution of simulated JJA mean all-sky DRF of BC in the five weakest and five strongest EASM years, averaged over 110–125 °E. We find largest ~~–~~BC-induced forcing at the latitude of ~~35~~30–40 °N in the weakest monsoon years and 35–40 °N in the strongest monsoon years. The shift of the center of the highest BC DRF~~ N;~~ is likely due to the different vertical distributions of BC concentrations between the weakest and strongest monsoon years (**Fig. 5a**). BC DRF is higher by >0.13 W $m^{-2}$ (10–20%) over 30–35 °N in the five weakest EASM years compared to the five strongest EASM years, which are consistently with those in **Fig. 8a**. A maximum BC DRF (>2 W $m^{-2}$) is shown approximately at an altitude of 3–10 km, because of the larger direct radiative forcing efficiency of BC at high altitude.

带格式的：字体：加粗

**Fig. 10a** shows the simulated vertical profiles of JJA BC mass concentrations (μg $m^{-3}$) averaged over eastern China for 1986–2006. The simulated BC concentrations are higher in MERRA than in GEOS-4 below 3 km. We find that the vertical profiles of JJA BC in GEOS-4 generally show larger interannual variations than those in MERRA. The variations of JJA BC in MERRA and in GEOS-4 range from –5% to 4% (–7% to 12%) at the surface, –25% to 16% (–23% to 23%) at 1 km, –35% to 42% (–32% to 46%) at 2 km, –23% to 32% (–25% to 67%) at 3 km, –13% to 10% (–18% to 71%) at 4 km, –10% to 7% (–14% to >76%) at 5–8 km. The differences in vertical profiles of BC in MERRA between the weakest and strongest EASM years (1998–1997) are –46% to 7%, with the largest differences of –0.09 μg $m^{-3}$ at ~2 km. We further compare the differences in simulated vertical profiles of JJA BC between the five weakest and five strongest EASM years averaged over northern and southern China in MERRA. The decreased BC concentrations throughout the troposphere in the weakest monsoon years lead to a reduction in the BC DRF in southern China (Table 4), while the increased BC concentrations below 2 km result in a significant increase of the BC DRF in northern China (Table 4).

Studies have shown that the impact of non-China emissions is significant on vertical profiles and hence DRF of BC in China; the contributions of non-China

emissions to concentrations and DRF of BC in China are larger than 20% at 5 km altitude and about 17–43%, respectively (e.g., Li et al., 2016). **Figure 11a** shows vertical distribution of simulated JJA mean all-sky DRF of BC due to non-China emissions in the five weakest and five strongest EASM years, averaged over 110–125 °E. Model results are from simulation VNOC, in which the anthropogenic and biomass burning emissions are turned off in China. The non-China emissions induce a high (> 0.16 W $m^{-2}$) BC DRF above ~5 km due to the significant contributions of non-China emissions to BC concentrations at high altitudes. Compared to the five strongest EASM years, the simulated DRF of BC due to non-China emissions in the weakest EASM years is larger (by ~10%) at 25–40 °N, because of the higher (by > 10%) BC concentrations transported to the region (**Fig. 12a**).

# 4 Impact of EAWM on Interannual Variation of BC

## 4.1 Simulated DJF BC in GEOS-4 and MERRA

Simulated DJF surface BC concentrations averaged over eastern China also have strong interannual variations, ranging from 1.30–1.58 μg $m^{-3}$ (–8.9 to 10.8%) in GEOS-4 for 1986–2006 and from 2.05–2.31 μg $m^{-3}$ (–7.0% to 5.2%) in MERRA for 1980–2010 (**Fig. 1b**). DJF mean surface concentrations of BC for 1986–2006 are 0.77 μg $m^{-3}$ (54%) higher in MERRA than in GEOS-4. Again, the consistently stronger precipitation in GEOS-4 (by 0.3 mm $d^{-1}$, 21% on average) largely accounts for the lower surface BC concentrations (**Figs. 1S** and **2a**). The DJF mean precipitation averaged for 1986–2006 is higher in GEOS-4 than in MERRA in most of China (**Fig. 1S**), except in the delta of the Yangtze River in eastern China. The resulting differences in BC wet deposition between GEOS-4 and MERRA show similar patterns as those in precipitation (not shown). The DJF mean wet deposition of BC in GEOS-4 is generally higher (by 0.007 kg $s^{-1}$, 5% on average) than that in MERRA for 1986–2006, except in 1998 (**Fig. 2b**). In addition, we find that the planetary boundary layer height (PBLH) partially accounts for the abovementioned differences in surface BC concentrations between GEOS-4 and MERRA. The DJF mean PBLH is generally

higher in GEOS-4 than in MERRA by 11.6 m (2%, **Fig. ~~not shown~~S2**). The lower PBLH in MERRA suppresses the convection and thus leads to higher BC concentrations in the surface ~~.~~

带格式的：字体：加粗

### 4.2 Correlation between DJF BC and EAWMI

**Fig. 1b** shows the normalized EAWMI and simulated DJF mean surface BC concentrations averaged over eastern China from simulation VMET for 1980–2010 and from VMETG4 for 1986–2006. The correlation coefficient between the surface BC concentrations and the EAWMI_GEOS4 is –0.7 for 1986–2006, and those between surface BC and the EAWMI_MERRA are –0.6 and –0.7, respectively, for 1980–2010 and for 1986–2006. Different definitions of the EAWMI also show negative correlations with simulated DJF surface BC concentrations (Table 1, $r$ = –0.16 to –0.72). This negative correlation between simulated DJF mean surface BC concentrations and the EAWMIs over eastern China indicates that surface BC concentrations are generally high in the weak winter monsoon years. The correlation coefficients in GEOS-4 and MERRA show similar spatial distribution and magnitude; negative correlations are found in most of China, while positive correlations are over southwestern China (**Fig. 3b**).

### 4.3 Differences in BC between Weak and Strong EAWM years

**Fig. 4b** shows the differences in simulated DJF mean surface BC concentrations (μg $m^{-3}$) between weakest (1990, 1993, 1997, 1998, and 2002) and strongest (1986, 1996, 2001, 2005, and 2006) EAWM years during 1986–2006 from model simulations using the GEOS-4 and MERRA data. The spatial distribution of the differences in concentrations is in good agreement with the distribution of the correlation coefficients between the EAWMI and surface BC (**Fig. 3b)**. In eastern China, DJF surface BC concentrations in GEOS-4 are 0.12 μg $m^{-3}$ (9%) higher in the weakest winter monsoon years than in the strongest years (Table 2). The

corresponding values are 0.11 μg $m^{-3}$ (5%) higher in MERRA. In northern China, simulated surface BC concentrations are higher in the weakest monsoon years than in the strongest monsoon year by 0.13 μg $m^{-3}$ (8%) in GEOS-4 and by 0.14 μg $m^{-3}$ (5%) in MERRA. In southern China, the corresponding concentrations are higher by 0.10 μg $m^{-3}$ (12%) and 0.04 μg $m^{-3}$ (3%), respectively, in GEOS-4 and in MERRA. The difference in surface BC concentrations between the weakest and strongest winter monsoon years over each region is significant by comparing with the corresponding mean and standard deviation of DJF mean surface BC for 1986–2006 (Table 2). We find that the region over 30–40 ° N has lower BC concentrations in the weakest monsoon years. This lower concentrations are also shown in **Fig. 5b**, which represents the height-latitude of differences in simulated DJF mean BC concentrations between the five weakest and five strongest EAWM years during 1986–2006 and averaged over 110–125 ° E from model simulations VMETG4 and VMET. Increased BC concentrations in the weakest monsoon years are found over north of 20 ° N in both GEOS-4 and MERRA, except the region over 30–40 °N and above 1 km.

The changes in atmospheric circulation again likely account for the increased BC concentrations in the weak winter monsoon years in eastern China. **Fig. 6b** shows the composite differences in DJF 850 hPa wind (m $s^{-1}$) between the five weakest and five strongest EAWM years from the GEOS-4 and MERRA data. The differences in wind in GEOS-4 show a similar pattern as those in MERRA. In DJF, northerly winds are weaker in the weaker monsoon years than in the stronger monsoon years. As a result, anomalous southwesterlies are found in the weakest monsoon years along the coast of eastern China and anomalies southeasterlies control northern China and northeast China, which do not favor the outflow of pollutants from eastern China (Table 3). Fig. **7b** shows the differences in simulated upward mass flux of DJF BC (kg $s^{-1}$) between the five weakest and five strongest EAWM years. The differences are averaged over the longitude range of 110–125 ° E. Compared to the strongest monsoon years, increases in upward mass flux of BC concentrations are found over 20–30 ° N and north of 40 ° N in the troposphere in the weakest monsoon years, confirming the increased surface BC concentrations in northern and southern China (**Figs. 4b** and **5b**).

We find decreased upward transport of BC over 30–40 °N in the weakest monsoon years, which is consistent with decreased concentrations in the region of static winds (**Fig. 6b**). Our results are consistent with the studies, e.g., Li et al. (2015) and Zhou et al. (2015), which showed that the change in wind speed and wind direction is the major factor of the negative correlation between the increased winter fog–haze days and the weaken of the EAWM in China.

We further summarize~~y~~ in Table 3 the differences in horizontal fluxes of DJF BC at the four lateral boundaries of the northern and southern boxes (**Fig. 4b**, from the surface to 10 km) between the five weakest and five strongest EAWM years, based on simulations VMETG4 and VMET. Both northern and southern China show increased BC concentrations in the weakest monsoon years than in the strongest monsoon years (**Fig. 4b**). In the southern box, we find larger inflow of BC by 1.67 (0.99) kg $s^{-1}$ at the west boundary, less inflow by 1.45 (1.19) kg $s^{-1}$ at north boundary, less outflow by 0.52 (0.70) kg $s^{-1}$ at the south boundary, and larger outflow by 0.55 (0.10) kg $s^{-1}$ at east boundary, from simulation VMETG4 (VMET). The net effect in southern China is a larger inflow of BC by 0.19 (0.40) kg $s^{-1}$ in the weakest ~~monsoon~~ EAWM years than in the strongest EAWM ~~monsoon~~ years, which leads to the higher BC concentrations in the weakest EAWM years. As we discussed in Sect. 3.3, the larger outflow fluxes of BC by 0.09 (0.27) kg $s^{-1}$ result in the lower BC concentrations in southern China in the weakest EASM years than in the strongest EASM years. Different patterns of atmospheric circulation between summer and winter monsoon thus lead to the different distributions of BC in southern China.~~.~~ In northern China, there is a net effect of larger inflow of BC by 0.64 (0.62) kg $s^{-1}$ because of the anomalous southerlies and westerlies in the weakest monsoon years. The anomalous southerlies in northern China thus prevent the outflow of pollutants and lead to an increase in BC concentrations in the region in the weakest monsoon years. Compared to the strongest EAWM years, enhanced wet deposition of BC are found in the weakest monsoon years in both northern and southern China (Table 2), likely because of the increased BC concentrations and precipitation in the corresponding regions. Weaker upward transport in the weakest monsoon years than the strongest years

above 1-2 km in southern China (Fig. **7b**) is also not a dominate factor that contributes to the higher surface BC concentrations in the region (Tables 2 and 3).

带格式的：字体：加粗

### 4.4 Impact of EAWM on Vertical Profile and DRF of BC

**Fig. 8b** shows the simulated DJF mean all-sky TOA DRF of BC in the five weakest and strongest EAWM years during 1986–2006, based on simulation VMET. The simulated BC DRF is high in eastern China, with the largest values (> 5.0 W $m^{-2}$) in the Sichuan Basin. In northern China, the TOA DRF of BC is 0.03 W $m^{-2}$ (2%, Table 4) higher in the weakest monsoon years than in the strongest monsoon years, consistent to the higher BC concentrations in the region (**Fig. 4b**). We further separate northern China into two regions, the central China Plain (110–125 °E, 28–36 °N) and the northern China Plain (110–125 ° E, 37–45 ° N). Relative to the five strongest monsoon years, the BC DRF in the weakest monsoon years is higher in the northern China Plain by 0.11 W $m^{-2}$ (11%) but lower in the central China Plain by 0.03 W $m^{-2}$ (1%). In the central China Plain, although the surface concentrations are higher by 0.08 μg $m^{-3}$ (2%) in the weakest monsoon years, the corresponding DRF is lower partially because of the lower column burdens of tropospheric BC (by 0.04 mg $m^{-2}$, 1%, from surface to 10 km, Figs. 5(b right) and 10(b2)). In southern China, the DRF is 0.03 W $m^{-2}$ (3%) lower in the weakest monsoon years than in the strongest monsoon years. In contrast, both surface concentrations (higher by 0.04 μg $m^{-3}$, 3%) and column burdens (higher by 0.02 mg $m^{-2}$, 2%) of BC are higher in the weakest monsoon years. We attribute these discrepancies largely to the vertical distributions of BC concentrations as discussed in the following paragraph. We further compare in **Fig. 9b** the vertical distribution of simulated DJF DRF of BC in the five weakest and five strongest EAWM years, averaged over 110–125 °E. The BC-induced forcing is large (>2.8 W $m^{-2}$) at the latitude of 20–40 °N and at an altitude of 5–10 km. BC DRF is higher by > 0.1 W $m^{-2}$ (> 10%) north of 35 °N in the five weakest EAWM years than in the five strongest EAWM years, consistent with those in **Fig. 8b**.

The abovementioned differences in spatial patterns of DRF and BC concentrations

are likely because of the vertical distributions of BC concentrations. In general, the simulated vertical profiles of DJF BC concentrations are higher in MERRA than in GEOS-4, but the interannual variations are larger in GEOS-4 than in MERRA (**Fig. 10b**). The variations of DJF BC in MERRA (GEOS-4) range from –7% to 5% (–9% to 11%) at the surface, –12% to 10% (–13% to 27%) at 1 km, –19% to 14% (–13% to 62%) at 2 km, –14% to 15% (–17% to 57%) at 3 km, –17% to 16% (–22% to 61%) at 4 km, –17% to >14% (–22% to >67%) at 5–8 km. We find that the differences in vertical profiles of BC in MERRA between the weakest and strongest EAWM years (1990–1996) are –0.08 to 0.2 μg $m^{-3}$ (–11% to 12%) below 10 km, with the largest differences at the surface and ~1.5 km. We further compare the differences in simulated vertical profiles of DJF BC mass concentrations between the five weakest and five strongest EAWM years from model simulation VMET, averaged over southern China, the central China plain, and the northern China Plain. Relative to the strongest monsoon years, decreased BC concentrations are found in the weakest monsoon years from 2 to 5 km in southern China and from 1 to 6 km in the central China Plain. The decreased BC concentrations above 1–2 km lead to the reduction in the DRF in the two regions. In contrast, the higher DRF of BC in the northern China Plain in the weakest monsoon years is because of the increased BC concentrations throughout the troposphere.

The lower concentrations above 1–2 km in the weakest monsoon years in southern China and the central Chin Plain are likely because of the weaker vertical convection at the corresponding altitudes in the weakest monsoon years than in the strongest monsoon years. We calculate the horizontal and vertical fluxes of BC in two boxes of southern China and the central China Plain from 1 to 6 km (Table 5). In vertical direction, the two boxes have upward fluxes in both lower and upper boundaries. Relative to the strongest monsoon years, the southern box has a net outflow of 0.07 kg $s^{-1}$ in the weakest monsoon years; the central China Plain shows a net downward flux of 0.11 kg $s^{-1}$. The corresponding net horizontal fluxes are relatively smaller, and about 0.03 kg $s^{-1}$ in southern China and 0.01 kg $s^{-1}$ in the central China Plain. The weaker vertical fluxes above 1–2 km in the weakest monsoon

years thus result in the lower BC concentrations ~~above 1 km and~~at the elevated altitudes therefore the reduction in the DRF in the two regions.

~~Figure~~ Fig. **11b** shows the vertical distribution of simulated DJF mean all-sky DRF of BC due to non-China emissions in the five weakest and five strongest EAWM years, averaged over 110–125 °E. The non-China emissions induce a high (> 0.35 W $m^{-2}$) BC DRF at 15–35 °N. We also find a higher (by >5%) DRF of BC north of 25 °N in the weakest EAWM years than in the strongest years, due to the larger BC concentrations at the low troposphere in the weakest EAWM years (**Fig. 12b**).

## 5. Summary and conclusions

We quantified the impacts of the EASM and EAWM on the interannual variations of mass concentrations and DRF of BC in eastern China for 1986–2006 and examined the relevant mechanisms. We conducted simulations with fixed anthropogenic and biomass burning emissions at the year 2010 levels and driven by GEOS-4 for 1986–2006 and by MERRA for 1980–2010.

We found that simulated JJA and DJF surface BC concentrations averaged over eastern China were higher in MERRA than in GEOS-4 by 0.30 μg $m^{-3}$ (44%) and 0.77 μg $m^{-3}$ (54%), respectively. Our analyses indicated that generally higher precipitation in GEOS-4 than in MERRA largely accounted for the differences in BC concentrations using the two meteorological fields.

In JJA, simulated BC concentrations showed interannual variations of –5% to 4% in MERRA (–7% to 12% in GEOS-4) at the surface and –35% to 42% in MERRA (–32% to >76% in GEOS-4) above 1 km. The differences in vertical profiles of BC between the weakest and strongest EASM years (1998–1997) reached up to –0.09 μg $m^{-3}$ (–46%) at 1–2 km. Simulated JJA surface BC concentrations negatively correlated with the strength of the EASM ($r$ = –0.7 in GEOS-4 and –0.4 in MERRA), mainly by the changes in atmospheric circulation. Relative to the five strongest

EASM years, simulated JJA surface BC concentrations in the five weakest EASM years were higher over northern China by 0.09 μg $m^{-3}$ (11%) in GEOS-4 and by 0.04 μg $m^{-3}$ (3%) in MERRA. The corresponding concentrations were lower over southern China by 0.03 μg $m^{-3}$ (11%) and 0.04 μg $m^{-3}$ (10%). The resulting JJA mean TOA DRF of BC were 0.04 W $m^{-2}$ (3%) higher in northern China but 0.06 W $m^{-2}$ (14%) lower in southern China.

In DJF, the changes in meteorological parameters alone led to interannual variations in BC concentrations ranging from –7% to 5% in MERRA (–9% to 11% in GEOS-4) at the surface and –19% to >14% in MERRA (–22% to >67% in GEOS-4) above 1 km. Simulated DJF surface BC concentrations negatively correlated with the EAWMI ($r$ = –0.7 in GEOS-4 and –0.7 in MERRA), indicating higher DJF surface BC concentrations in the weaker EAWM years. We also found that the changes in atmospheric circulation likely accounted for the increased BC concentrations in the weak EAWM years. In winter, anomalous southerlies in the weak monsoon years did not favor the outflow of pollutants, leading to an increase in BC concentration. Compared to the five strongest EAWM years, simulated DJF surface BC concentrations in the five weakest EAWM years were higher in northern China by 0.13 μg $m^{-3}$ (8%) in GEOS-4 and 0.14 μg $m^{-3}$ (5%) in MERRA. The corresponding concentrations were also higher in southern China by 0.10 μg $m^{-3}$ (12%) and 0.04 μg $m^{-3}$ (3%). The resulting TOA DRF of DJF BC was 0.03 W $m^{-2}$ (2%) higher in northern China but 0.03 W $m^{-2}$ (2%) lower in southern China. In southern China, the decreased BC concentrations above 1–2 km in the weakest EAWM years led to the reduction in BC DRF, likely due to the weaker vertical convection in the corresponding altitudes. The vertical profiles of BC are lower in weakest EAWM year (1990) than in the strongest year (1996) above 1–2 km, with the largest values of –0.08 μg $m^{-3}$ (–11%) in eastern China.

Different patterns of atmospheric circulation between summer and winter monsoon lead to the different distributions of BC in southern and northern China. Note that these different changes in BC concentrations and DRF between northern and southern China due to the EAM would be useful for proposing efficient air

带格式的：字体：非倾斜

quality regulation in different regions of China. It is also worth to point out that the BC DRF is also dependent on factors such as cloud and background aerosol distributions (Samset et al., 2011), which can be influenced by the strength of the EAM (Liu et al., 2010; Zhu et al., 2012). In addition, the strength of the EAWM would influence the following summer monsoon via changes in the factors such as circulation and precipitation (e.g., Chen et al., 2000), and further affect the aerosols concentrations and radiative forcing. These aspects should be further investigated in future studies.

带格式的：字体：非倾斜，字体颜色：自动设置
带格式的：字体颜色：自动设置
带格式的：字体：非倾斜，字体颜色：自动设置
带格式的：字体颜色：自动设置
带格式的：字体：非倾斜，字体颜色：自动设置
带格式的：缩进：首行缩进： 0 字符

*Acknowledgements.* This work was supported by the National Basic Research Program of China (973 program, Grant 2014CB441202), the Strategic Priority Research Program of the Chinese Academy of Sciences Strategic Priority Research Program Grant No. XDA05100503, the National Natural Science Foundation of China under grants 91544219, 41475137, and 41321064. The GEOS-Chem model is managed by the Atmospheric Chemistry Modeling group at Harvard University with support from the NASA ACMAP program.

带格式的：行距：单倍行距

## References

Allen, D. J., Rood, R. B., Thompson, A. M., and Hudson, R. D.: Three-dimensional ranon 222 calculations using assimilated metrological data and a convective mixing algorithm, J. Geophys. Res., 101, 6871–6881, 1996a.

Allen, D. J., Kasibhatla, P., Thompson, A. M., Rood, R. B., Doddridge, B. G., Pickering, K. E., Hudson, R. D., and Lin, S.-J.: Transport-induced interannual variability of carbon monoxide determined using a chemistry and transport model, J. Geophys. Res., 101, 28655–28669, 1996b.

Arakawa, A., and Schubert, W. H.: Interaction of a cumulus cloud ensemble with the large-scale environment, Part I, J. Atmos. Sci., 31, 674–701, 1974.

Bey, I., Jacob, D. J., Yantosca, R. M., Logan, J. A., Field, B. D., Fiore, A. M., Li, Q., Liu, H. Y., Mickley, L. J., and Schultz, M. G.: Global modeling of tropospheric chemistry with assimilated meteorology: Model description and evaluation, J. Geophys. Res. Atmos., 106 (D19), 23073–23095, doi:10.1029/2001JD000807, 2001.

Bollasina, M. A., Ming, Y., and Ramaswamy, V.: Anthropogenic aerosols and the weakening of the South Asian summer monsoon, Science, 334(6055), 502–505, doi:10.1126/science.1204994, 2011.

Bond, T. C., Streets, D. G., Yarber, K. F., Nelson, S. M., Woo, J.-H., and Klimont, Z.: A technology-based global inventory of black and organic carbon emissions from combustion, J. Geophys. Res. Atmos., 109(D14), D14203, doi:10.1029/2003JD003697, 2004.

Bond, T. C., Bhardwaj, E., Dong, R., Jogani, R., Jung, S., Roden, C., Streets, D. G., and Trautmann, N. M.: Historical emissions of black and organic carbon aerosol from energy-related combustion, 1850–2000, Global Biogeochem. Cycles, 21, GB2018, 2007.

Bond, T. C., Doherty, S. J., Fahey, D. W., Forster, P. M., Berntsen, T., DeAngelo, B. J., Flanner, M. G., Ghan, S., Kärcher, B., Koch, D., Kinne, S., Kondo, Y., Quinn, P. K., Sarofim, M. C., Schultz, M. G., Schulz, M., Venkataraman, C., Zhang, H., Zhang, S., Bellouin, N., Guttikunda, S. K., Hopke, P. K., Jacobson, M. Z., Kaiser, J. W., Klimont, Z., Lohmann, U., Schwarz, J. P., Shindell, D., Storelvmo, T., Warren, S. G., and Zender, C. S.: Bounding the role of black carbon in the climate system: scientific assessment, J. Geophys. Res. Atmos., 118 (11), 5380–5552, doi:10.1002/jgrd.50171, 2013.

Chang, C.-P., Zhang, Y., and Li, T: Interannual and interdecadal variations of the East Asian summer monsoon and tropical Pacific SSTs, Part I: Roles of the subtropical ridge, J. Clim., 13(24), 4310–4325, doi:10.1175/1520-0442(2000)013<4310:IAIVOT>2.0.CO;2, 2000.

Chen, H., and Wang, H.: Haze Days in North China and the associated atmospheric circulations based on daily visibility data from 1960 to 2012, Journal of Geophysical Research: Atmospheres, 120, doi:10.1002/2015JD023225, 2015.

Chen, W., Graf, H., and Ronghui, H.: The interannual variability of East Asian Winter Monsoon and its relation to the summer monsoon, Adv. Atmos. Sci., 17, 48–60, doi:10.1007/s00376-000-0042-5, 2000.

Chin, M., Ginoux, P., Kinne, S., Torres, O., Holben, B. N., Duncan, B. N., Martin, R. V., Logan, J. A., Higurashi, A., and Nakajima, T.: Tropospheric aerosol optical thickness from the GOCART model and comparisons with satellite and sun photometer measurements, J. Atmos. Sci., 59, 461–483, 2002.

Cooke, W. F., Liousse, C., Cachier, H., and Feichter, J.: Construction of a 1° × 1° fossil fuel emission data set for carbonaceous aerosol and implementation and radiative impact in the ECHAM4 model, J. Geophys. Res. Atmos., 104 (D18), 22137–22162, doi:10.1029/1999JD900187, 1999.

Ding, Y., Wang, Z., and Sun, Y.: Inter-decadal variation of the summer precipitation in east China and its association with decreasing Asian summer monsoon, Part I: Observed evidences, Int. J. Climatol., 28(9), 1139–1161, doi:10.1002/joc.1615, 2008.

Drury, E., Jacob, D. J., Spurr, R. J. D., Wang, J., Shinozuka, Y., Anderson, B. E., Clarke, A. D., Dibb, J., McNaughton, C., and Weber, R.: Synthesis of satellite (MODIS), aircraft (ICARTT), and surface (IMPROVE, EPA-AQS, AERONET)

aerosol observations over eastern North America to improve MODIS aerosol retrievals and constrain surface aerosol concentrations and sources, J. Geophys. Res. Atmos., 115 (D14), doi:10.1029/2009JD012629, 2010.

Gu, Y., Liou, K. N., Chen, W., and Liao, H.: Direct climate effect of black carbon in China and its impact on dust storms, J. Geophys. Res., 115, D00K14, doi:10.1029/2009JD013427, 2010.

Guo, Q.: Relationship between the variability of East Asia winter monsoon and temperature amomalies in China, Q. J. Appl. Meteorol., 5, 218-225, 1994 (in Chinese).

Hack, J. J.: Parameterization of moist convection in the NCAR community climate model (CCM2), J. Geophys. Res., 99, 5551–5568, 1994.

Heald, C. L., Ridley, D. A., Kroll, J. H., Barrett, S. R. H., Cady-Pereira, K. E., Alvarado, M. J., and Holmes, C. D.: Contrasting the direct radiative effect and direct radiative forcing of aerosols, Atmos. Chem. Phys., 14(11), 5513-5527, doi: 10.5194/acp-14-5513-2014, 2014.

Intergovernmental Panel on Climate Change (IPCC), Climate Change 2013: The Physical Science Basis. Contribution of Working Group I to the Fifth Assessment Report of the Intergovernmental Panel on Climate Change, edited by: Stocker, T.F., Qin, D., Plattner, G.-K., Tignor, M., Allen, S. K., Boschung, J., Nauels, A., Xia, Y., Bex, V., and Midgley, P. M., Cambridge University Press, Cambridge, United Kingdom and New York, NY, USA, 1535 pp, 2013.

Jacobson, M. Z.: Strong radiative heating due to the mixing state of black carbon in atmospheric aerosols, Nature, 409, 695–697, 2001.

Jeong, J. I., and Park, R. J.: Effects of the meteorological variability on regional air quality in East Asia, Atmos. Environ., 69, 46–55, doi:10.1016/J.Atmosenv.2012.11.061, 2013.

Jhun, J.-G., and Lee, E.-J.: A New East Asian Winter Monsoon Index and Associated Characteristics of the Winter Monsoon, J. Clim., 17, 711–726, doi:10.1175/1520-0442(2004)017<0711:ANEAWM>2.0.CO;2, 2004.

Ji, L., Sun, S., Arpe, K., and Bengtsson, L.: Model study on the interannual variability of Asian winter monsoon and its influence, Adv. Atmos. Sci., 14, 1-22, doi: 10.1007/s00376-997-0039-4, 1997.

Kalnay, E., Kanamitsu, M., Kistler, R., Collins, W., Deaven, D., Gandin, L., Iredell, M., Saha, S., White, G., Woollen, J., Zhu, Y., Leetmaa, A., Reynolds, R., Chelliah, M., Ebisuzaki, W., Higgins, W., Janowiak, J., Mo, K. C., Ropelewski, C., Wang, J., Jenne, R., and Joseph, D.: The NCEP/NCAR 40-Year Reanalysis Project, Bull. Amer. Meteor. Soc., 77, 437–471, doi:10.1175/1520-0477(1996)077<0437:TNYRP>2.0.CO;2, 1996.

Kurokawa, J., Ohara, T., Morikawa, T., Hanayama, S., Janssens-Maenhout, G., Fukui, T., Kawashima, K., and Akimoto, H.: Emissions of air pollutants and greenhouse gases over Asian regions during 2000–2008: Regional Emission inventory in Asia (REAS) version 2, Atmos. Chem. Phys., 13, 11019–11058, doi:10.5194/acp-13-11019-2013, 2013.

Lau, K. M., M. K. Kim, and K. M. Kim, 2006: Asian summer monsoon anomalies

带格式的: 题注, 缩进: 左侧: 0 厘米, 悬挂缩进: 2 字符, 首行缩进: -2 字符

带格式的: 不检查拼写或语法

带格式的: 题注, 缩进: 左侧: 0 厘米, 悬挂缩进: 2 字符, 首行缩进: -2 字符

带格式的: 不检查拼写或语法

induced by aerosol direct forcing: The role of the Tibetan Plateau, Climate Dyn., 26**,** 855–864.
Li, J., and Zeng, Q.: A unified monsoon index, Geophys. Res. Lett., 29, 115-1–115-4, doi:10.1029/2001GL013874, 2002.
Li, K., Liao, H., Mao, Y. H., and Ridley, D. A.: Sectoral and Regional Contributions to Black Carbon and its Direct Radiative Forcing in China, Atmos. Environ., 124, 351–366, doi:10.1016/j.atmosenv.2015.06.014, 2016.
Li, Q., Zhang, R., and Wang, Y.: Interannual variation of the wintertime fog–haze days across central and eastern China and its relation with East Asian winter monsoon, Int. J. Climatol., doi: 10.1002/joc.4350, 2015.
Lin, S.-J., and Rood, R. B.: Multidimensional flux-form semi-Lagrangian transport schemes, Mon. Weather Rev., 124, 2046–2070, 1996.
Liu, H., Jacob, D. J., Bey, I., and Yantosca, R. M.: Constraints from 210Pb and 7Be on wet deposition and transport in a global three-dimensional chemical tracer model driven by assimilated meteorological fields, J. Geophys. Res. Atmos., 106(D11), 12109–12128, doi:10.1029/2000JD900839, 2001.
Liu, X., Yan, L., Yang, P., Yin, Z.-Y., and North, G. R.: Influence of Indian Summer Monsoon on Aerosol Loading in East Asia, J. Appl. Meteor. Climatol., 50, 523–533, doi:10.1175/2010JAMC2414.1, 2010.
Lu, Z., Zhang, Q., and Streets, D. G.: Sulfur dioxide and primary carbonaceous aerosol emissions in China and India, 1996–2010, Atmos. Chem. Phys., 11(18), 9839–9864, doi:10.5194/acp-11-9839-2011, 2011.
Mao, Y. H., Liao, H., Han, Y., and Cao, J.: Impacts of meteorological parameters and emissions on decadal and interannual variations of black carbon in China for 1980–2010, J. Geophys. Res. Atmos., 121, 1822–1843, doi:10.1002/2015JD024019, 2016.
Meehl, G. A., Arblaster, J. M., and Collins, W. D.: Effects of black carbon aerosols on the Indian monsoon, Journal of Climate, 21, 2869–2882, DOI: 10.1175/2007JCLI1777.1, 2008.
Menon, S., Hansen, J., Nazarenko, L., and Luo, Y.: Climate effects of black carbon aerosols in China and India, Science, 297, 2250–2253, 2002.
Moorthi, S., and Suarez, M. J.: Relaxed Arakawa-Schubert: A parameterization of moist convection for general circulation models, Mon. Wea. Rev., 120, 978–1002, 1992.
Mu, Q., and Liao, H.: Simulation of the interannual variations of aerosols in China: role of variations in meteorological parameters, Atmos. Chem. Phys., 14, 9597–9612, doi:10.5194/acp-14-9597-2014, 2014.
Niu, F., Li, Z., Li, C., Lee, K., and Wang, M.: Increase of wintertime fog in China: Potential impacts of weakening of the Eastern Asian monsoon circulation and increasing aerosol loading, J. Geophys. Res., 115, D00K20, 2010.
Ohara T., Akimoto, H., Kurokawa, J., Horii, N., Yamaji, K., Yan, X., and Hayasaka, T.: An Asian emission inventory of anthropogenic emission sources for the period 1980–2020, Atmos. Chem. Phys., 7, 4419–4444, 2007.
Park, R. J., Jacob, D. J., Chin, M., and Martin, R. V.: Sources of carbonaceous

aerosols over the United States and implications for natural visibility, J. Geophys. Res. Atmos., 108 (D12), 4355, doi: 10.1029/2002JD003190, 2003.

Park, R. J., Jacob, D. J., Palmer, P. I., Clarke, A. D., Weber, R. J., Zondlo, M. A., Eisele, F. L., Bandy, A. R., Thornton, D. C., Sachse, G. W., and Bond, T. C.: Export efficiency of black carbon aerosol in continental outflow: global implications, J. Geophys. Res. Atmos., 110 (D11), D11205, doi:10.1029/2004JD005432, 2005.

Qin, Y., and Xie, S. D.: Spatial and temporal variation of anthropogenic black carbon emissions in China for the period 1980–2009, Atmos. Chem. Phys., 12(11), 4825-4841, doi:10.5194/acp-12-4825-2012, 2012.

Qu, W., Wang, J., Zhang, X., Yang, Z., and Gao, S.: Effect of cold wave on winter visibility over eastern China, J. Geophys. Res. Atmos., 120, 2394–2406, doi:10.1002/2014JD021958, 2015.

Ramanathan, V., and Xu, Y. Y.: The Copenhagen Accord for limiting global warming: Criteria, constraints, and available avenues, P. Natl. Acad. Sci. USA, 107(18), 8055–8062, doi:10.1073/pnas.1002293107, 2010.

~~Ramanathan, V., and Carmichael, G.: Global and regional climate changes due to black carbon, Nature Geosci., 1 (4), 221–227, doi:10.1038/ngeo156, 2008.~~

Rienecker, M. M., Suarez, M. J., Gelaro, R., Todling, R., Bacmeister, J., Liu, R., Bosilovich, M. G., Schubert, S. D., Takacs, L., Kim, G-K, Bloom, S., Chen, J., Collins, D., Conaty, A., da Silva, A., Gu, W., Joiner, J., Koster, R. D., Lucchesi, R., Molod, A., Owens, T., Pawson, S., Pegion, P., Redder, C. R., Reichle, R., Robertson, F. R., Ruddick, A. G., Sienkiewicz, M., and Woollen, J.: MERRA: NASA's Modern-Era Retrospective Analysis for Research and Applications, J. Climate, 24, 3624–3648, doi:10.1175/JCLI-D-11-00015.1, 2011.

Samset, B. H., Myhre, G., Schulz, M., Balkanski, Y., Bauer, S., Berntsen, T. K., Bian, H., Bellouin, N., Diehl, T., Easter, R. C., Ghan, S. J., Iversen, T., Kinne, S., Kirkevåg, A., Lamarque, J. F., Lin, G., Liu, X., Penner, J. E., Seland, Ø., Skeie, R. B., Stier, P., Takemura, T., Tsigaridis, K., and Zhang, K.: Black carbon vertical profiles strongly affect its radiative forcing uncertainty, Atmos. Chem. Phys., 13(5), 2423-2434, doi:10.5194/acp-13-2423-2013, 2013.

Shindell, D., Kuylenstierna, J. C. I., Vignati, E., van Dingenen, R., Amann, M., Klimont, Z., Anenberg, S. C., Muller, N., Janssens-Maenhout, G., Raes, F., Schwartz, J., Faluvegi, G., Pozzoli, L., Kupiainen, K., Höglund-Isaksson, L., Emberson, L., Streets, D., Ramanathan, V., Hicks, K., Oanh, N. T. K., Milly, G., Williams, M., Demkine, V., and Fowler, D.: Simultaneously Mitigating Near-Term Climate Change and Improving Human Health and Food Security, Science, 335(6065), 183–189, doi:10.1126/science.1210026, 2012.

Smith, S. J., and Mizrahi, A.: Near-term climate mitigation by short-lived forcers, Proceedings of the National Academy of Sciences, 110(35), 14202–14206, doi:10.1073/pnas.1308470110, 2013.

Van der Werf, G. R., Randerson, J. T., Giglio, L., Collatz, G. J., Mu, M., Kasibhatla, P. S., Morton, D. C., DeFries, R. S., Jin, Y., and van Leeuwen, T. T.: Global fire

带格式的：默认段落字体，字体：(默认) +西文正文 (Calibri)，(中文) +中文正文 (宋体)，五号

emissions and the contribution of deforestation, savanna, forest, agricultural, and peat fires (1997–2009), Atmos. Chem. Phys., 10(23), 11707–11735, doi:10.5194/acp-10-11707-2010, 2010.

Walcek, C. J., Brost, R. A., and Chang, J. S.: $SO_2$, sulfate, and $HNO_3$ deposition velocities computed using regional land use and meteorological data, Atmos. Environ, 20, 949–964, 1986.

Wang, L., Huang, R., Gu, L., Chen, W., and Kang, L.: Interdecadal Variations of the East Asian Winter Monsoon and Their Association with Quasi-Stationary Planetary Wave Activity, J. Clim., 22, 4860–4872, doi:10.1175/2009JCLI2973.1, 2009.

Wang, L., Zhang, N., Liu, Z., Sun, Y. Ji, D. and Wang, Y.: The Influence of Climate Factors, Meteorological Conditions, and Boundary-Layer Structure on Severe Haze Pollution in the Beijing-Tianjin-Hebei Region during January 2013, Advances in Meteorology, 685971, doi:10.1155/2014/685971, 2014.

Wang, Q., Jacob, D. J., Fisher, J. A., Mao, J., Leibensperger, E. M., Carouge, C. C., Le Sager, P., Kondo, Y., Jimenez, J. L., Cubison, M. J., and Doherty, S. J.: Sources of carbonaceous aerosols and deposited black carbon in the Arctic in winter-spring: implications for radiative forcing, Atmos. Chem. Phys., 11(23), 12453–12473, doi:10.5194/acp-11-12453-2011, 2011.

Wang, R., Tao, S., Wang, W., Liu, J., Shen, H., Shen, G., Wang, B., Liu, X., Li, W., Huang, Y., Zhang, Y., Lu, Y., Chen, H., Chen, Y., Wang, C., Zhu, D., Wang, X., Li, B., Liu, W., and Ma, J.: Black carbon emissions in China from 1949 to 2050, Environ. Sci. Technol., 46(14), 7595–7603, doi:10.1021/es3003684, 2012.

Wu, B., and Wang, J.: Winter Arctic Oscillation, Siberian High and East Asian Winter Monsoon, Geophys. Res. Lett., 29, 1897, doi:10.1029/2002gl015373, 2002.

Xu, Y., Bahadur, R., Zhao, C., and Leung, L. R.: Estimating the radiative forcing of carbonaceous aerosols over California based on satellite and ground observations, Journal of Geophysical Research: Atmospheres, 118(19), 11148–11160, doi:10.1002/jgrd.50835, 2013.

Yan, H., Zhou, W., Yang, H., and Cai, Y.: Definition of an East Asian Winter Monsoon Index and Its Variation Characteristics, Transactions of Atmospheric Sciences, 32(3), 367–376, 2009 (in Chinese).

Yan, L., Liu, X., Yang, P., Yin, Z.-Y., and North, G. R.: Study of the Impact of Summer Monsoon Circulation on Spatial Distribution of Aerosols in East Asia Based on Numerical Simulations, J. Appl. Meteor. Climatol., 50, 2270–2282, doi:10.1175/2011JAMC-D-11-06.1, 2011.

Yang, Y., Liao, H., and Li, J.: Impacts of the East Asian summer monsoon on interannual variations of summertime surface-layer ozone concentrations over China, Atmos. Chem. Phys., 14, 6867–6880, doi:10.5194/acp-14-6867-2014, 2014.

Yang, Y., Liao, H., and Lou, S.: Decadal trend and interannual variation of outflow of aerosols from East Asia: Roles of variations in meteorological parameters and emissions, Atmos. Environ., 100, 141–153, 2015.

Yin, Z., Wang, H., and Guo, W.: Climatic change features of fog and haze in winter over North China and Huang-huai Area, Science China Earth Sciences, doi: 10.1007/s11430-015-5089-3, 2015.

带格式的：字体：非倾斜
带格式的：字体：非倾斜
带格式的：字体：非倾斜
带格式的：字体：非倾斜
带格式的：字体：非倾斜
带格式的：字体：非倾斜
带格式的：不检查拼写或语法

Zhang, G. J., and McFarlane, N. A.: Role of convective-scale momentum transport in climate simulation, J. Geophys. Res., 100, 1417–1426, doi:10.1029/94JD02519, 1995.

Zhang, L., Liao, H., and Li, J.: Impact of the Southeast Asian summer monsoon strength on the outflow of aerosols from South Asia, Ann. Geophys., 28, 277–287, 2010a.

Zhang, L., Liao, H., and Li, J.: Impacts of Asian summer monsoon on seasonal and interannual variations of aerosols over eastern China, J. Geophys. Res. Atmos., 115(D7), D00K05, doi:10.1029/2009JD012299, 2010b.

Zhang, X. Y., Wang, Y. Q., Zhang, X. C., Guo, W., and Gong, S. L.: Carbonaceous aerosol composition over various regions of China during 2006, J. Geophys. Res. Atmos., 113 (D14), D14111, doi:10.1029/2007JD009525, 2008.

Zhang, X. Y., Wang, Y. Q., Niu, T., Zhang, X. C., Gong, S. L., Zhang, Y. M., and Sun, J. Y.: Atmospheric aerosol compositions in China: spatial/temporal variability, chemical signature, regional haze distribution and comparisons with global aerosols, *Atmos. Chem. Phys.*, 12, 779–799, doi:10.5194/acp-12-779-2012, 2012.

Zhang, Y., Ding, A., Mao, H., Nie, W., Zhou, D., Liu, L., Huang, X., and Fu, C.: Impact of synoptic weather patterns and inter-decadal climate variability on air quality in the North China Plain during 1980–2013, Atmospheric Environment, 124B, 119–128, 2016.

Zhou, W., Tie, X., Zhou, G., and Liang, P.: Possible effects of climate change of wind on aerosol variation during winter in Shanghai, China, Particuology, 20, 80–88, doi:10.1016/j.partic.2014.08.008, 2015.

Zhu, J., Liao, H., and Li, J.: Increases in aerosol concentrations over eastern China due to the decadal-scale weakening of the East Asian summer monsoon, Geophys. Res. Lett., 39, L09809, doi:10.1029/2012GL051428, 2012.

**Tables and Figures**

**Table 1.** Correlation coefficients among different definitions of the strength of the East Asian winter monsoon (EAWM), and between the EAWM Index (EAWMI) and simulated December-January-February (DJF) mean surface BC concentrations averaged over eastern China (110–125 ° E, 20–45 ° N). Simulated BC concentrations are from model simulations VMETG4 and VMET, and corresponding monsoon indexes are calculated based on GEOS-4 and MERRA assimilated meteorological data.

**Table 2**. Simulated JJA (DJF) mean surface BC concentrations (μg $m^{-3}$) in the five weakest and five strongest EASM (EAWM) years during 1986–2006. Results are from simulations VMETG4 and VMET averaged over northern China (NC, 110–125 °E, 28–45 °N), southern China (SC, 110–125 °E, 20–27 ° N), and eastern China (EC, 110–125 °E, 20–45 °N).

**Table 3**. The composite analyses of JJA (DJF) horizontal fluxes of BC (kg $s^{-1}$) for two selected boxes (northern China (110–125 ° E, 28–45 ° N) and southern China (110–125 ° E, 20–27 ° N), from the surface to 10 km) based on simulations VMETG4 and VMET. The values are averages over the five weakest and five strongest EASM (EAWM) years during 1986–2006. For horizontal fluxes, positive values indicate eastward or northward transport and negative values indicate westward or southward transport. Also shown are the corresponding wet deposition of BC (kg $s^{-1}$) for the two selected boxes.

**Table 4**. Simulated JJA (DJF) mean all-sky direct radiative forcing (DRF) of BC (W $m^{-2}$) at the top of the atmosphere (TOA) in the five weakest and five strongest EASM (EAWM) years during 1986–2006. Results are from simulation VMET averaged over eastern China (110–125 ° E, 20–45 ° N), northern China (110–125 °E, 28–45 °N), the northern China Plain (110–125 ° E, 37–45 °N), the central China Plain (110–125 °E, 28–36 °N), and southern China (110–125 °E, 20–27 °N).

**Table 5**. The composite analyses of DJF horizontal and vertical fluxes of BC (kg $s^{-1}$) for two selected boxes (the central China Plain (110–125 °E, 27–36 °N) and southern China (110–125 ° E, 20–27 ° N), from 1 to 6 km) based on simulation VMET. The values are averages over the five weakest and five strongest EAWM years during 1986–2006. For fluxes, positive values indicate eastward, northward, or upward transport and negative values indicate westward, southward, or downward transport.

**Figure 1. (a)** Normalized East Asian summer monsoon Index (EASMI, bars, left y axis) and the simulated June-July-August (JJA) mean surface BC concentrations (lines, right y axis, μg $m^{-3}$) averaged over eastern China (20–45 °N, 110–125 °E) from model simulation VMET (red line) for 1980–2010 and from VMETG4 (blue line) for 1986–2006. EASMI are calculated based on MERRA (red bars) and GEOS-4 (blue bars) assimilated

meteorological data following Li and Zeng (2002). **(b)** Same as **(a)**, but for normalized East Asian winter monsoon Index (EAWMI) and the simulated December-January-February (DJF) mean surface BC concentrations. EAWMIs are calculated following Wu and Wang (2002).

**Figure 2. (a)** JJA and DJF mean precipitation (mm $d^{-1}$) averaged over eastern China for 1986–2006 from GEOS-4 (blue lines) and MERRA (red lines) meteorological data. DJF mean precipitation is multiplied by 5 in **(a2)**. **(b)** Same as **(a)**, but for wet deposition (kg $s^{-1}$).

**Figure 3. (a)** Correlation coefficients between EASMI and JJA mean surface BC concentrations during 1986–2006. **(b)** Correlation coefficients between EAWMI and DJF mean surface BC concentrations during 1986–2006. Simulated BC concentrations are from model simulations VMETG4 (left) and VMET (right), and monsoon indexes are calculated based on GEOS-4 (left) and MERRA (right) assimilated meteorological data. The dotted areas indicate statistical significance with 95% confidence from a two-tailed Student's t test.

**Figure 4. (a1)** Absolute (μg $m^{-3}$) and **(a2)** percentage (%) differences in simulated JJA mean surface BC concentrations between weakest (1988, 1993, 1995, 1996, and 1998) and strongest (1990, 1994, 1997, 2004, and 2006) EASM years during 1986–2006 from model simulations VMETG4 and VMET. **(b1)** and **(b2)** Same as **(a1)** and **(a2)**, respectively, but for absolute (μg $m^{-3}$) and percentage (%) differences in simulated DJF mean surface BC concentrations between weakest (1990, 1993, 1997, 1998, and 2002) and strongest (1986, 1996, 2001, 2005, and 2006) EAWM years. The enclosed areas are defined as northern China (NC, 110–125 ° E, 28–45 ° N) and southern China (SC, 110–125 °E, 20–27 °N).

**Figure 5. (a)** Height-latitude cross section of differences in simulated JJA mean BC concentrations (μg $m^{-3}$) between the five weakest and five strongest EASM years during 1986–2006. Plots are averaged over longitude range of 110–125 ° E from model simulations VMETG4 (left) and VMET (right). **(b)** Same as **(a)**, but for differences in DJF between five weakest and five strongest EAWM years.

**Figure 6. (a)** Differences in JJA 850 hPa wind (vector, m $s^{-1}$) between the five weakest and five strongest EASM years during 1986–2006 from GEOS-4 (left) and MERRA (right) data. **(b)** Same as **(a)**, but for differences in DJF wind between five weakest and five strongest EAWM years.

**Figure 7. (a)** Differences in simulated upward mass flux of JJA BC (kg $s^{-1}$) between the five weakest and five strongest EASM years during 1986–2006. Plots are averaged over longitude range of 110–125 ° E from model simulations

VMETG4 (left) and VMET (right). **(b)** Same as **(a)**, but for differences in DJF between five weakest and five strongest EAWM years.

**Figure 8. (a)** Simulated JJA mean all-sky direct radiative forcing (DRF) of BC (W $m^{-2}$) at the top of the atmosphere (TOA) in the **(a1)** five weakest and **(a2)** five strongest EASM years during 1986–2006 from model simulation VMET. Also shown are the **(a3)** absolute (W $m^{-2}$) and **(a4)** percentage (%) differences between the five weakest and five strongest EASM years. **(b)** Same as **(a)**, but for simulated DJF mean all-sky TOA DRF of BC in the five weakest and five strongest EAWM years. The enclosed areas are defined as northern China (NC, 110–125 °E, 28–45 °N), the northern China Plain (NCP, 110–125 ° E, 36–45 ° N), the central China Plain (CCP, 110–125 °E, 28–36 °N), and southern China (SC, 110–125 °E, 20–27 °N).

**Figure 9. (a)** Height-latitude cross sections of simulated JJA mean all-sky DRF of BC (W $m^{-2}$) in the **(a1)** five weakest and **(a2)** five strongest EASM years during 1986–2006. Also shown are the **(a3)** absolute (W $m^{-2}$) and **(a4)** percentage (%) differences between the five weakest and five strongest EASM years. Plots are averaged over longitude range of 110–125 °E from model simulation VMET. **(b)** Same as **(a)**, but for simulated DJF mean all-sky DRF of BC in the five weakest and five strongest EAWM years.

**Figure 10. (a1)** Simulated vertical profiles of JJA BC mass concentrations (μg $m^{-3}$) averaged over 1986–2006. The error bars represent the minimum and maximum values of BC. Results are averages over eastern China from model simulations VMETG4 (blue) and VMET (red). **(a2)** Differences in simulated vertical profiles of JJA BC mass concentrations (μg $m^{-3}$) between the five weakest and five strongest EAM years (solid lines) during 1986–2006, and between the weakest and strongest EASM years (1998–1997, dotted lines)**.** Results are averages over eastern China, northern China, and southern China from model simulations VMET. **(b1)** Same as **(a1),** but for simulated DJF BC mass concentrations. **(b2)** Same as **(a2),** but for differences in DJF between the five weakest and five strongest EAWM years and between the weakest and strongest EAWM years (1990–1996). Results are averages over eastern China, northern China Plain, the central China Plain, and southern China.

**带格式的：** 字体：（中文）宋体

**Figure ~~11~~11.** Same as **Figure 9,** but for the contributions from non-China emissions to simulated all-sky DRF of BC.

**Figure ~~12~~12. (a)** Height-latitude cross sections of contributions of non-China emissions to simulated JJA mean BC concentrations (μg $m^{-3}$) in the **(a1)** five weakest and **(a2)** five strongest EASM years during 1986–2006. Also shown are the **(a3)** absolute (μg $m^{-3}$) and **(a4)** percentage (%) differences between the five weakest and five strongest EASM years. Plots are averaged over longitude range of 110–125 ° E from model simulation

**带格式的：** 缩进：悬挂缩进：9.95 字符，左 −0.01 字符，定义网格后自动调整右缩进，段落间距段后：10 磅，孤行控制，调整中文与西文文字的间距，调整中文与数字的间距，制表位： 0 字符，左对齐

VMET. **(b)** Same as **(a)**, but for simulated DJF mean BC concentrations in the five weakest and five strongest EAWM years

**Figure 1S.** JJA and DJF mean precipitation (mm $d^{-1}$) averaged for 1986–2006 from GEOS-4 **(a)** and MERRA **(b)** meteorological data. Also shown are the differences between GEOS-4 and MERRA data **(c)**.

**Figure 2S. (left)** Differences in DJF mean planetary boundary layer height (PBLH, m) averaged for 1986–2006 between GEOS-4 and MERRA. **(right)** DJF mean PBLH averaged over eastern China for 1986–2006 from GEOS-4 (blue line) and MERRA (red line).

**带格式的：** 缩进：悬挂缩进：9.95 字符，左 -0.01 字符，定义网格后自动调整右缩进，段落间距段后：10 磅，孤行控制，调整中文与西文文字的间距，调整中文与数字的间距，制表位： 0 字符，左对齐

**带格式的：** 字体：(中文) TimesNewRomanPS-BoldMT，加粗

**Table 1.** Correlation coefficients among different definitions of the strength of the East Asian winter monsoon (EAWM), and between the EAWM Index (EAWMI) and simulated December-January-February (DJF) mean surface BC concentrations averaged over eastern China (110–125 °E, 20–45 °N). Simulated BC concentrations are from model simulations VMETG4 and VMET, and corresponding monsoon indexes are calculated based on GEOS-4 and MERRA assimilated meteorological data.

| Correlation | GEOS–4 (1986-2006) | | MERRA (1986-2006) | | MERRA (1980-2010) | |
|---|---|---|---|---|---|---|
| | EAWMI[1] | BC | EAWMI | BC | EAWMI | BC |
| EAWMI_$T$[2] | 0.63 | –0.57 | 0.58 | –0.16 | 0.56 | –0.29 |
| EAWMI_$V$[3] | 0.51 | –0.31 | 0.56 | –0.50 | 0.54 | –0.40 |
| EAWMI_$U$[4] | 0.77 | –0.42 | 0.82 | –0.72 | 0.73 | –0.69 |
| EAWMI_$P_1$[5] | 0.65 | –0.33 | 0.72 | –0.38 | 0.77 | –0.41 |
| EAWMI_$P_2$[6] | 0.71 | –0.61 | 0.72 | –0.68 | 0.70 | –0.66 |

[1]$\mathrm{EAWMI}_i = \mathrm{norm}(\sum_{20°\mathrm{N}}^{70°\mathrm{N}}(P_{1i}-P_{2i}))$, $P_{1i}$ is the DJF mean sea level pressure over 110 °E, $P_{2i}$ is the DJF mean sea level pressure over 160 °E (Wu and Wang, 2002).

[2]EAWMI_$T_i = \bar{\bar{T}} - \bar{T}_i$, $\bar{T}_i$ is the DJF mean surface temperature over the region of 20–40 °N and 110–135 °E for year $i$, $\bar{\bar{T}}$ is the mean of $\bar{T}_i$ (Yan et al., 2009).

[3]EAWMI_$V_i = \bar{\bar{V}} - \bar{V}_i$, $\bar{V}_i$ is the DJF mean 850 hpa meridional wind over the region of 20–40 °N and 110–135 °E for year $i$, $\bar{\bar{V}}$ is the mean of $\bar{V}_i$ (Yan et al., 2009).

[4]EAWMI_$U_i = \overline{U_{1i}} - \overline{U_{2i}}$, $\overline{U_{1i}}$ is the DJF mean 300 hpa zonal wind over the region of 27.5–37.5 °N and 110–170 °E for year *i*, $\overline{U_{2i}}$ is the DJF mean 300 hpa zonal wind over the region of 50–60 °N and 80–140 °E for year *i* (Jhun et al., 2004).

[5]EAWMI_$P_{1i} = \overline{P_{1i}} - \overline{P_{2i}}$, $\overline{P_{1i}}$ is the DJF mean sea level pressure over the region of 30–55 °N and 110–130 °E for year *i*, $\overline{P_{2i}}$ is the DJF mean sea level pressure over the region of 20–40 °N and 150–180 °E for year *i* (Yan et al., 2009).

[6]EAWMI_$P_{2i} = \overline{P_{1i}}$, $\overline{P_{1i}}$ is the DJF mean sea level pressure over the region of 40–60 °N and 80–120 °E for year *i* (Yan et al., 2009).

**Table 2**. Simulated JJA (DJF) mean surface BC concentrations (μg $m^{-3}$) in the five weakest and five strongest EASM (EAWM) years during 1986–2006. Results are from simulations VMETG4 and VMET averaged over northern China (NC, 110–125 °E, 28–45 °N), southern China (SC, 110–125 °E, 20–27 °N), and eastern China (EC, 110–125 °E, 20–45 °N).

带格式表格

| Month | Region | Surface Concentrations of BC (μg $m^{-3}$) | | | | | |
|---|---|---|---|---|---|---|---|
| | | GEOS-4 | | | MERRA | | |
| | | Weak | Strong | Difference[a] | Weak | Strong | Difference |
| JJA | southern China | 0.24 | 0.27 | -0.03 (-11%) | 0.37 | 0.41 | -0.04 (-10%) |
| | northern China | 0.94 | 0.85 | 0.09 (11%) | 1.30 | 1.26 | 0.04 (3%) |
| | eastern China | 0.72 | 0.67 | 0.05 (9%) | 1.02 | 1.00 | 0.02 (2%) |
| DJF | southern China | 0.90 | 0.80 | 0.10 (12%) | 1.14 | 1.10 | 0.04 (3%) |
| | northern China | 1.76 | 1.63 | 0.13 (8%) | 2.76 | 2.62 | 0.14 (5%) |
| | eastern China | 1.37 | 1.50 | -0.12 (-9%) | 2.26 | 2.15 | 0.11 (5%) |

| Month | Region | Surface Concentrations of BC (μg m$^{-3}$) | | | | | | | | | |
|---|---|---|---|---|---|---|---|---|---|---|---|
| | | GEOS-4 | | | | | MERRA | | | | |
| | | Weak | Strong | Diff.[a] | Mean[b] | Std.[c] | Weak | Strong | Diff. | Mean | Std. |
| JJA | SC | 0.24 | 0.27 | –0.03 (–11%) | 0.26 | 0.02 | 0.37 | 0.41 | –0.04 (–10%) | 0.39 | 0.02 |
| | NC | 0.94 | 0.85 | 0.09 (11%) | 0.89 | 0.05 | 1.30 | 1.26 | 0.04 (3%) | 1.27 | 0.03 |
| | EC | 0.72 | 0.67 | 0.05 (9%) | 0.70 | 0.03 | 1.02 | 1.00 | 0.02 (2%) | 1.00 | 0.02 |
| DJF | SC | 0.90 | 0.80 | 0.10 (12%) | 0.85 | 0.06 | 1.14 | 1.10 | 0.04 (3%) | 1.12 | 0.04 |
| | NC | 1.76 | 1.63 | 0.13 (8%) | 1.68 | 0.08 | 2.76 | 2.62 | 0.14 (5%) | 2.68 | 0.10 |
| | EC | 1.37 | 1.50 | 0.12 (9%) | 1.43 | 0.07 | 2.26 | 2.15 | 0.11 (5%) | 2.20 | 0.07 |

[a]The difference is (Weakest–Strongest) and the relative difference in percentage is in parentheses.

[b,c] The mean and the standard deviation of simulated JJA (DJF) mean surface BC concentrations for 1986–2006.

带格式表格
带格式的：右 -0.67 字符
带格式的：上标
带格式的：上标
带格式的：缩进：左 -0.5 字符，右 -0.67 字符
带格式的：上标
带格式的：缩进：左 -0.5 字符，右 -0.67 字符
带格式的：缩进：左 -0.5 字符，右 -0.67 字符
带格式的：缩进：左 -0.5 字符，右 -0.67 字符
带格式表格
带格式的：缩进：左 -0.5 字符，右 -0.67 字符
带格式的：缩进：左 -0.5 字符，右 -0.67 字符
带格式的：缩进：左 -0.5 字符，右 -0.67 字符
带格式的：上标
带格式的：字体：小五

**Table 3**. The composite analyses of JJA (DJF) horizontal fluxes of BC (kg s$^{-1}$) for two selected boxes (northern China (110–125 ° E, 28–45 ° N) and southern China (110–125 ° E, 20–27 ° N), from the surface to 10 km) based on simulations VMETG4 and VMET. The values are averages over the five weakest and five strongest EASM (EAWM) years during 1986–2006. For horizontal fluxes, positive values indicate eastward or northward transport and negative values indicate westward or southward

transport. Also shown are the corresponding wet deposition of BC (kg $s^{-1}$) for the two selected boxes.

| Boundary | GEOS-4 | | | MERRA | | |
|---|---|---|---|---|---|---|
| | Weakest | Strongest | Difference[a] | Weakest | Strongest | Difference[a] |
| | JJA, northern China (110–125 °E, 28–45 °N) | | | | | |
| South | +2.24 | +0.97 | +1.27 | +1.93 | +0.92 | +1.01 |
| North | +3.44 | +4.06 | –0.62 | +3.90 | +4.57 | –0.67 |
| West | +6.60 | +4.20 | +2.40 | +8.72 | +7.51 | +1.21 |
| East | +12.48 | +9.20 | +3.28 | +3.60 | +2.31 | +1.29 |
| Net | inflow 1.01 | | | inflow 1.60 | | |
| Deposition | 14.06 | 13.35 | 0.70 | 13.26 | 11.76 | 1.50 |
| ~~Net~~ | ~~inflow 1.01~~ | | | ~~inflow 1.60~~ | | |
| | JJA, southern China (110–125 °E, 20–27 °N) | | | | | |
| South | +0.62 | +0.70 | –0.08 | +0.61 | +0.60 | +0.01 |
| North | +1.79 | +0.88 | +0.91 | +1.67 | +0.95 | +0.72 |
| West | +0.94 | +0.13 | +0.81 | +0.47 | +0.12 | +0.35 |
| East | +0.33 | +0.42 | –0.09 | +0.18 | +0.27 | –0.09 |
| Net | outflow 0.09 | | | outflow 0.27 | | |
| Deposition | 2.46 | 3.02 | –0.56 | 2.26 | 2.84 | –0.58 |
| ~~Net~~ | ~~outflow 0.09~~ | | | ~~outflow 0.27~~ | | |
| | DJF, northern China (110–125 °E, 28–45 °N) | | | | | |
| South | –6.35 | –8.24 | +1.89 | –4.51 | –5.96 | +1.45 |
| North | –0.37 | –0.71 | +0.34 | +0.64 | –0.28 | +0.92 |
| West | +11.60 | +11.41 | +0.19 | +12.01 | +12.90 | –0.89 |

带格式表格

| | | | | | | |
|---|---|---|---|---|---|---|
| East | +22.77 | +21.67 | +1.10 | +23.55 | +24.53 | –0.98 |
| Net | inflow 0.64 | | | inflow 0.62 | | |
| Deposition | 9.48 | 9.24 | 0.24 | 9.17 | 8.75 | 0.42 |
| ~~Net~~ | ~~inflow 0.64~~ | | | ~~inflow 0.62~~ | | |
| | DJF, southern China (110–125 °E, 20–27 °N) | | | | | |
| South | –3.09 | –3.61 | +0.52 | –2.77 | –3.47 | +0.70 |
| North | –5.23 | –6.68 | +1.45 | –4.40 | –5.59 | +1.19 |
| West | +1.03 | –0.64 | +1.67 | +1.24 | +0.25 | +0.99 |
| East | +2.68 | +2.13 | +0.55 | +0.98 | +0.88 | +0.10 |
| Net | inflow 0.19 | | | inflow 0.40 | | |
| Deposition | 4.78 | 4.52 | 0.26 | 4.79 | 4.51 | 0.28 |
| ~~Net~~ | ~~inflow 0.19~~ | | | ~~inflow 0.40~~ | | |

[a]The difference is (Weakest–Strongest).

**Table 4**. Simulated JJA (DJF) mean all-sky direct radiative forcing (DRF) of BC (W $m^{-2}$) at the top of the atmosphere (TOA) in the five weakest and five strongest EASM (EAWM) years during 1986–2006. Results are from simulation VMET averaged over eastern China (110–125 °E, 20–45 °N), northern China (110–125 °E, 28–45 °N), the northern China Plain (110–125 °E, 37–45 °N), the central China Plain (110–125 °E, 28–36 °N), and southern China (110–125 °E, 20–27 °N).

| Month | Region | TOA DRF of BC, MERRA (W $m^{-2}$) | | |
|---|---|---|---|---|
| | | Weak | Strong | Difference[a] |
| JJA | southern China | 0.34 | 0.40 | –0.06 (14%) |
| | northern China | 1.41 | 1.38 | 0.04 (3%) |
| | eastern China | 1.08 | 1.07 | 0.01 (1%) |
| DJF | southern China | 1.04 | 1.07 | –0.03 (3%) |
| | northern China | 1.65 | 1.62 | 0.03 (2%) |
| | central China Plain | 2.11 | 2.14 | –0.03 (1%) |
| | northern China Plain | 1.08 | 0.97 | 0.11 (11%) |
| | eastern China | 1.46 | 1.45 | 0.01 (1%) |

[a]The difference is (Weakest–Strongest) and the relative difference in percentage is in parentheses.

**Table 5**. The composite analyses of DJF horizontal and vertical fluxes of BC (kg $s^{-1}$) for two selected boxes (the central China Plain (110–125 °E, 27–36 °N) and southern China (110–125 °E, 20–27 °N), from 1 to 6 km) based on simulation VMET. The values are averages over the five weakest and five strongest EAWM years during 1986–2006. For fluxes, positive values indicate eastward, northward, or upward transport and negative values indicate westward, southward, or downward transport.

| Boundary | Weakest | Strongest | Difference[a] | Net |
|---|---|---|---|---|
| | DJF, central China Plain (110–125 °E, 28–36 °N) | | | |
| South | +1.29 | +0.98 | +0.31 | Inflow 0.01 |
| North | +0.53 | +0.07 | +0.46 | |
| West | +7.84 | +8.89 | –1.05 | |
| East | +7.39 | +8.61 | –1.21 | |
| Upper | +0.99 | +1.24 | –0.25 | outflow 0.11 |
| Bottom | +5.22 | +5.56 | –0.34 | |
| | DJF, southern China (110–125 °E, 20–27 °N) | | | |
| South | –0.08 | –0.20 | +0.12 | inflow 0.03 |
| North | +0.91 | –0.67 | +0.24 | |
| West | +4.40 | +4.37 | +0.03 | |
| East | +1.70 | +1.82 | –0.12 | |
| Upper | +0.09 | +0.06 | +0.03 | outflow 0.07 |
| Bottom | +1.12 | +1.16 | –0.04 | |

[a]The difference is (Weakest–Strongest)

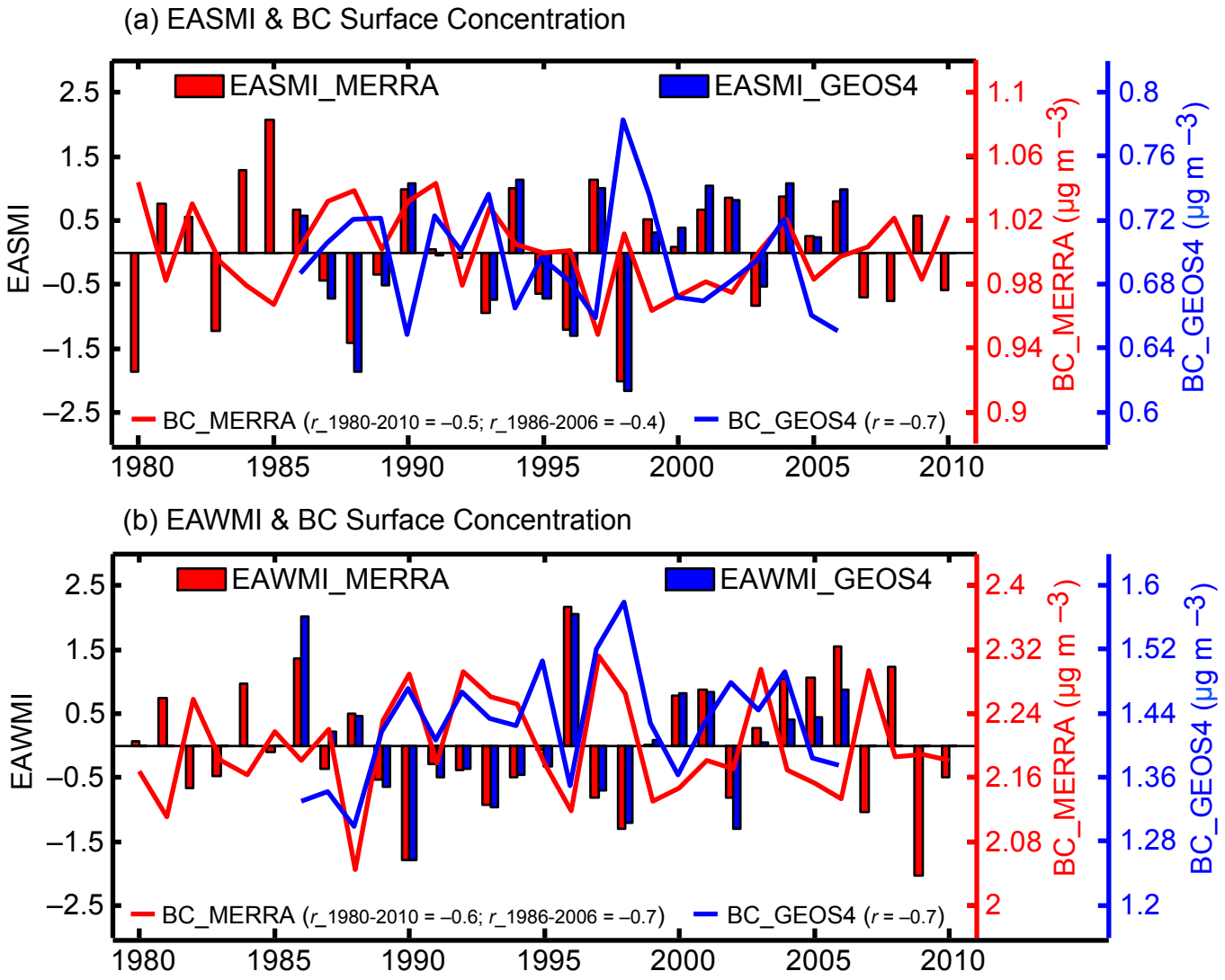


**Fig. 1. (a)** Normalized East Asian summer monsoon Index (EASMI, bars, left y axis) and the simulated June-July-August (JJA) mean surface BC concentrations (lines, right y axis, μg $m^{-3}$) averaged over eastern China (20–45° N, 110–125° E) from model simulation VMET (red line) for 1980–2010 and from VMETG4 (blue line) for 1986–2006. EASMI are calculated based on MERRA (red bars) and GEOS-4 (blue bars) assimilated meteorological data following Li and Zeng (2002). **(b)** Same as **(a)**, but for normalized East Asian winter monsoon Index (EAWMI) and the simulated December-January-February (DJF) mean surface BC concentrations. EAWMIs are calculated following Wu and Wang (2002).

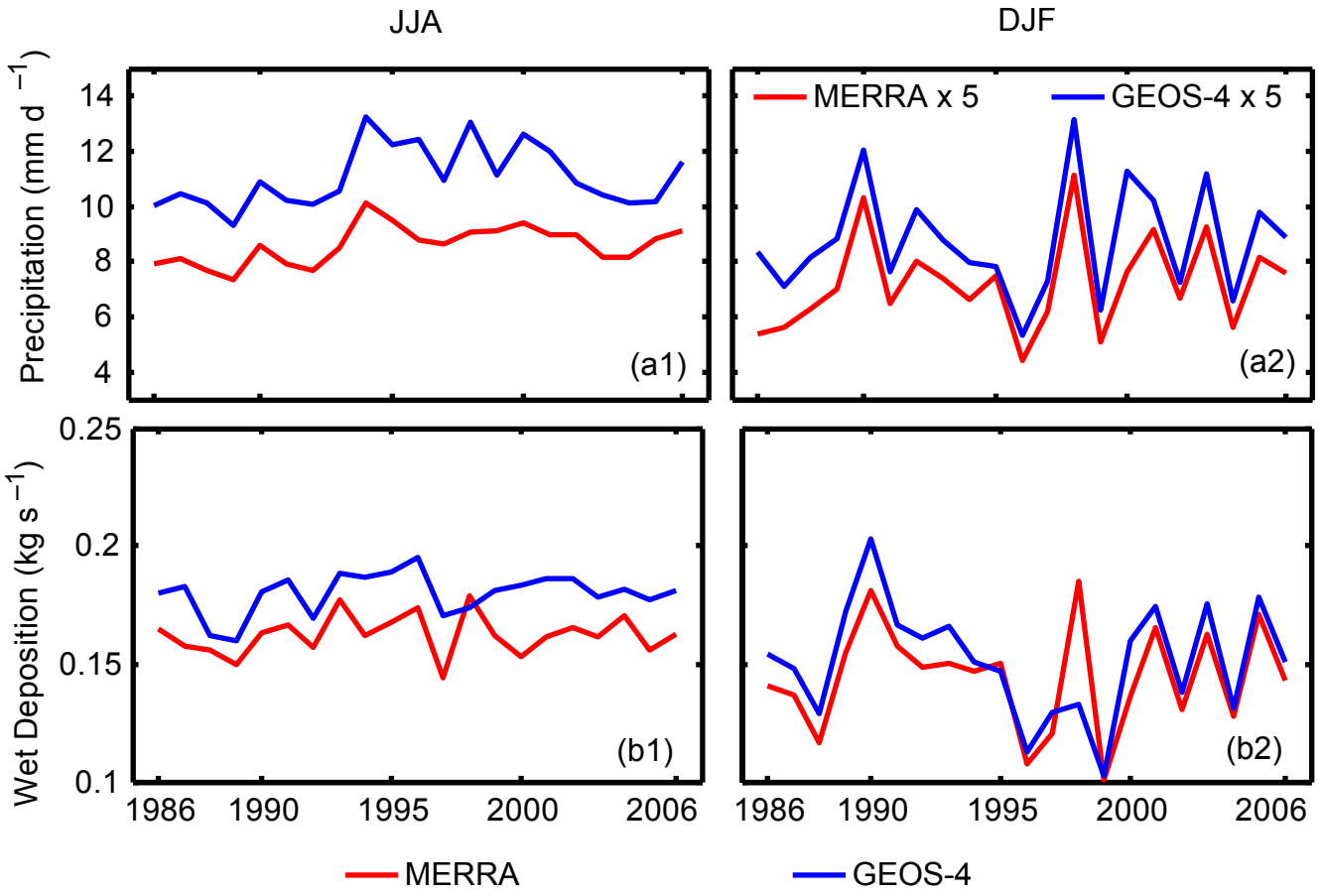


**Fig. 2. (a)** JJA and DJF mean precipitation (mm $d^{-1}$) averaged over eastern China for 1986–2006 from GEOS-4 (blue lines) and MERRA (red lines) meteorological data. DJF mean precipitation is multiplied by 5 in **(a2)**. **(b)** Same as **(a)**, but for wet deposition (kg $s^{-1}$).

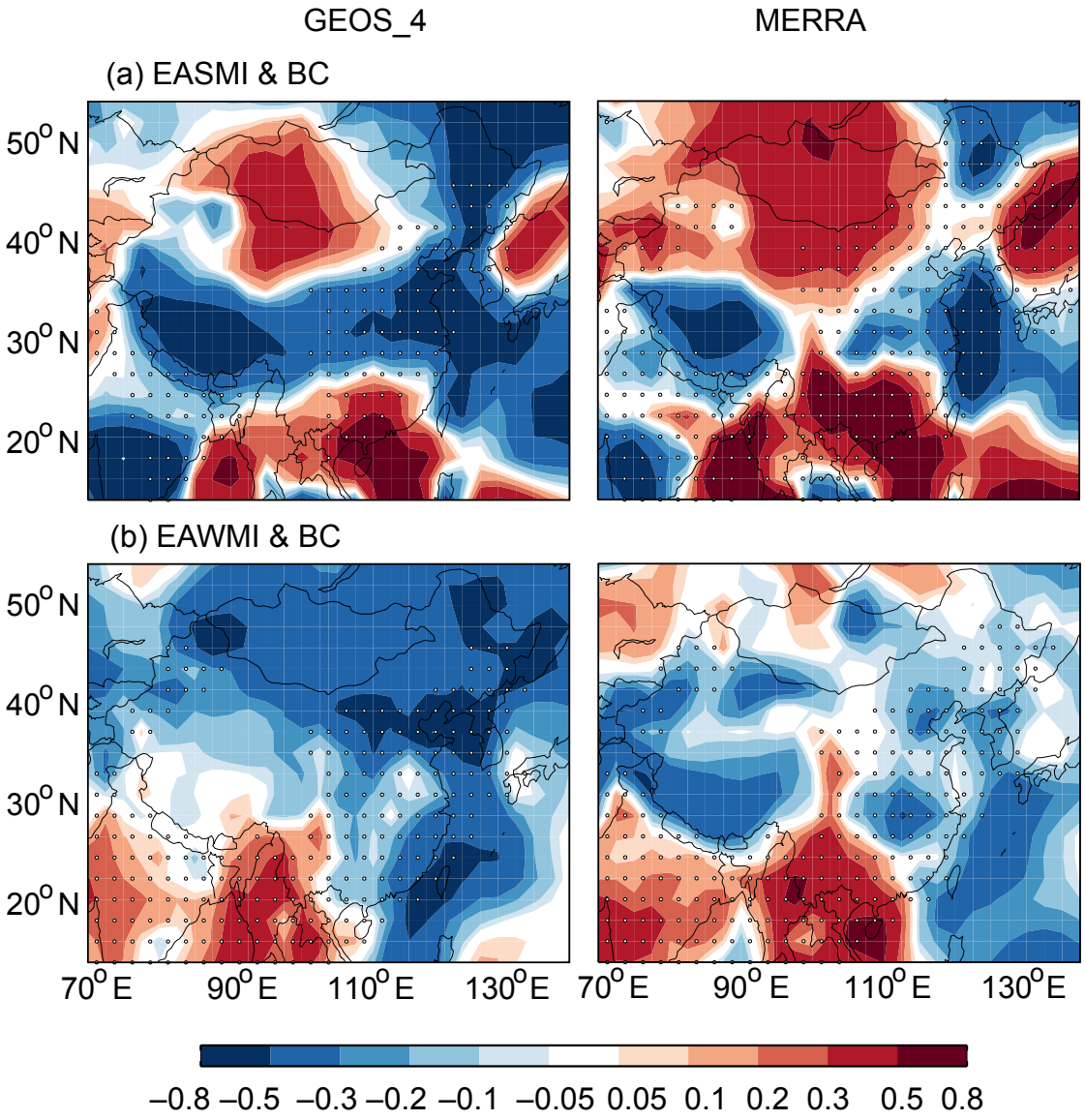


**Figure 3. (a)** Correlation coefficients between EASMI and JJA mean surface BC concentrations during 1986–2006. **(b)** Correlation coefficients between EAWMI and DJF mean surface BC concentrations during 1986–2006. Simulated BC concentrations are from model simulations VMETG4 (left) and VMET (right), and monsoon indexes are calculated based on GEOS-4 (left) and MERRA (right) assimilated meteorological data. The dotted areas indicate statistical significance with 95% confidence from a two-tailed Student's t test.

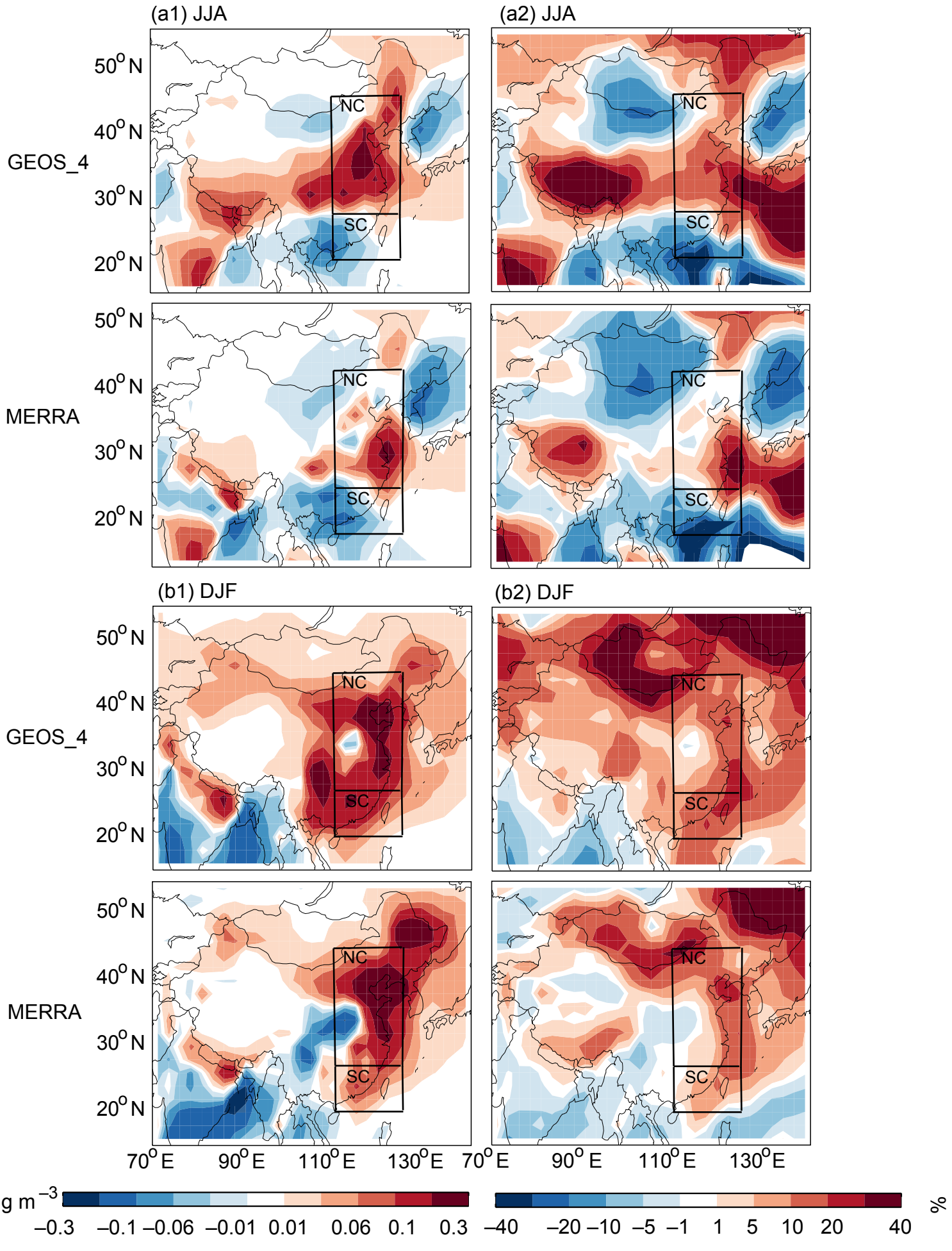
(a1) JJA
(a2) JJA
(b1) DJF
(b2) DJF
GEOS_4
MERRA
NC
SC
50° N
40° N
30° N
20° N
70° E
90° E
110° E
130° E
μg m −3
−0.3 −0.1 −0.06 −0.01 0.01 0.06 0.1 0.3
−40 −20 −10 −5 −1 1 5 10 20 40
%

**Fig. 4**

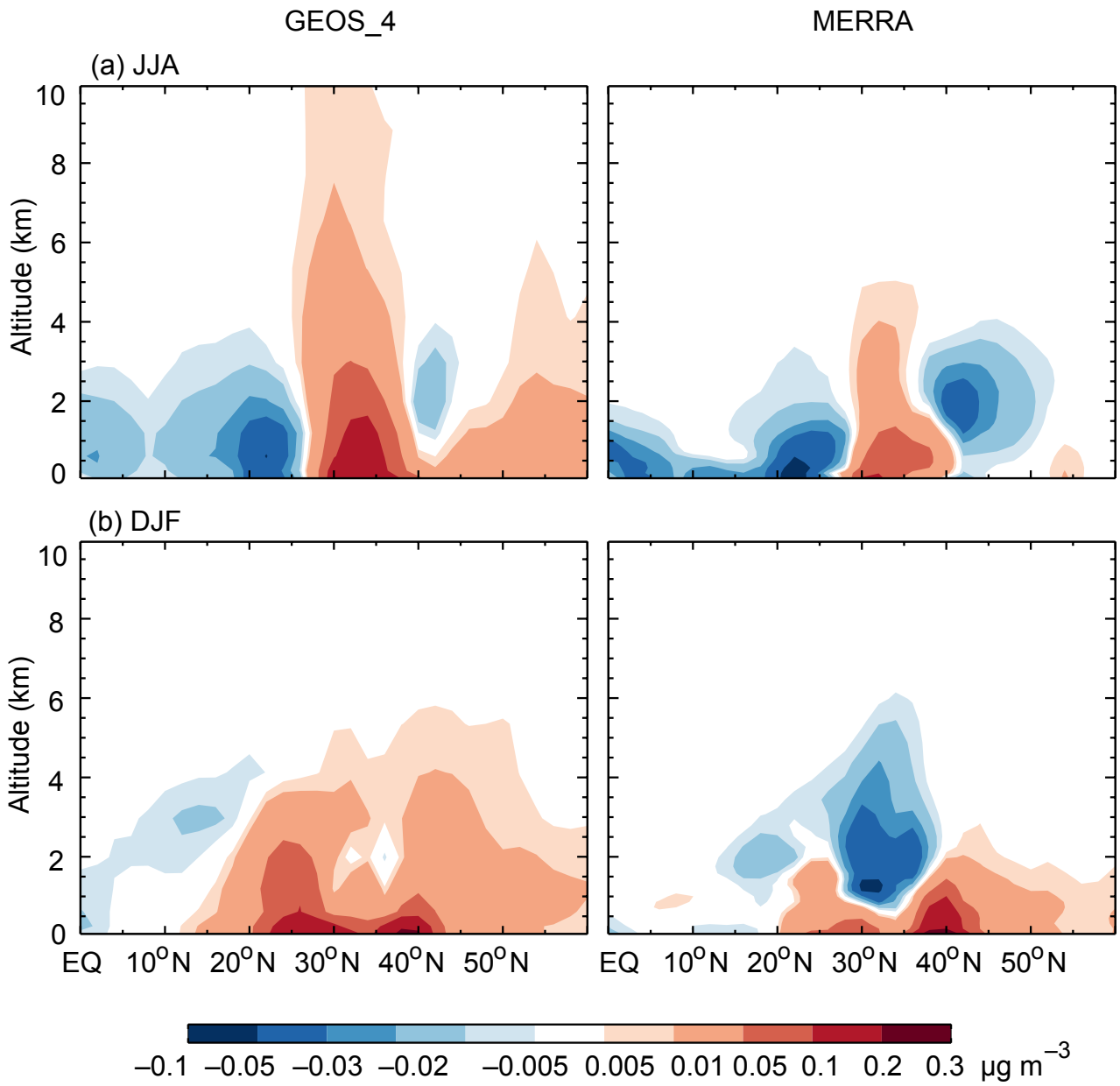


**Fig. 5. (a)** Height-latitude cross section of differences in simulated JJA mean BC concentrations (μg $m^{-3}$) between the five weakest and five strongest EASM years during 1986–2006. Plots are averaged over longitude range of 110–125° E from model simulations VMETG4 (left) and VMET (right). **(b)** Same as **(a)**, but for differences in DJF between five weakest and five strongest EAWM years.

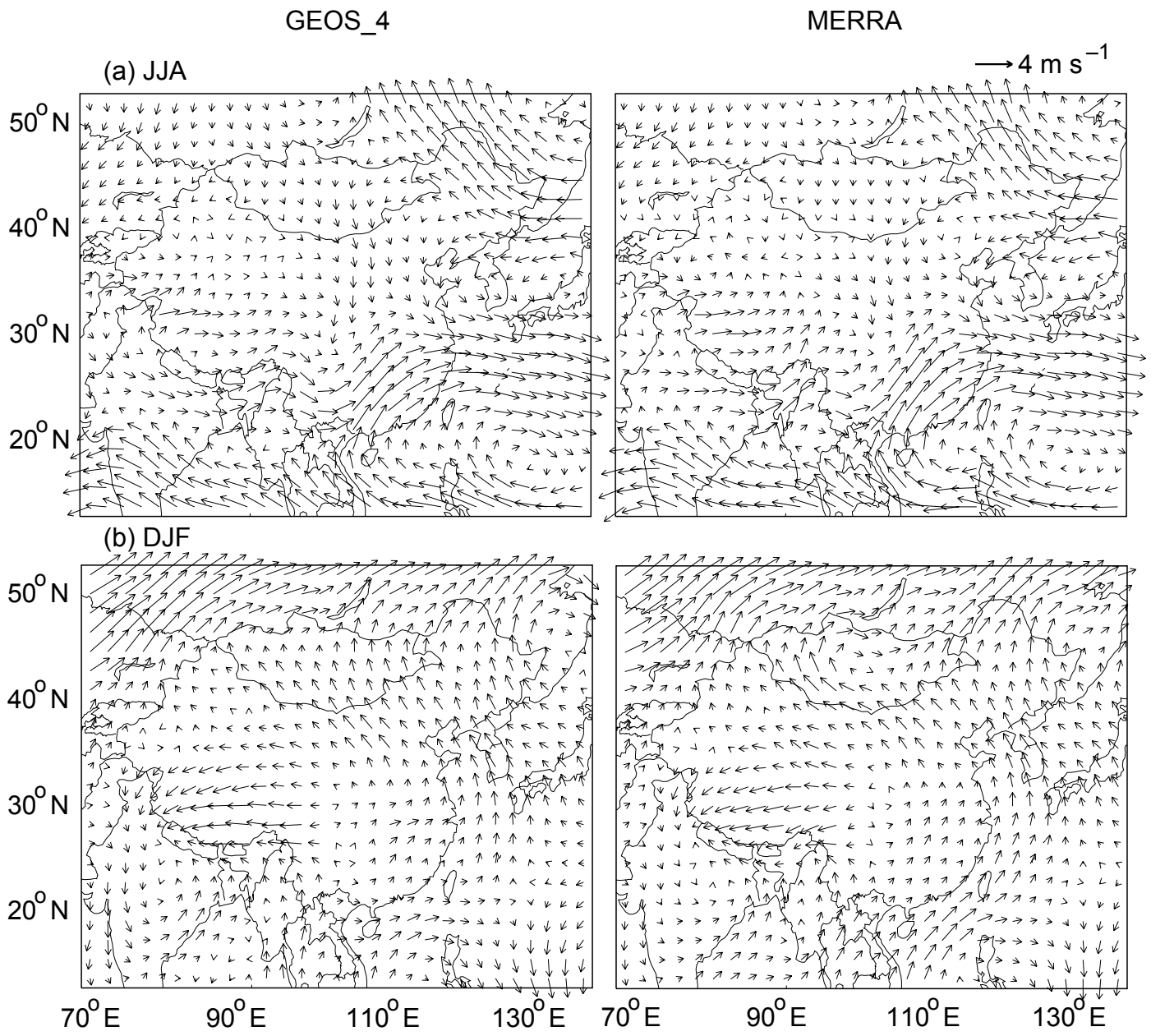


**Fig. 6. (a)** Differences in JJA 850 hPa wind (vector, m $s^{-1}$) between the five weakest and five strongest EASM years during 1986–2006 from GEOS-4 (left) and MERRA (right) data. **(b)** Same as **(a)**, but for differences in DJF wind between five weakest and five strongest EAWM years.

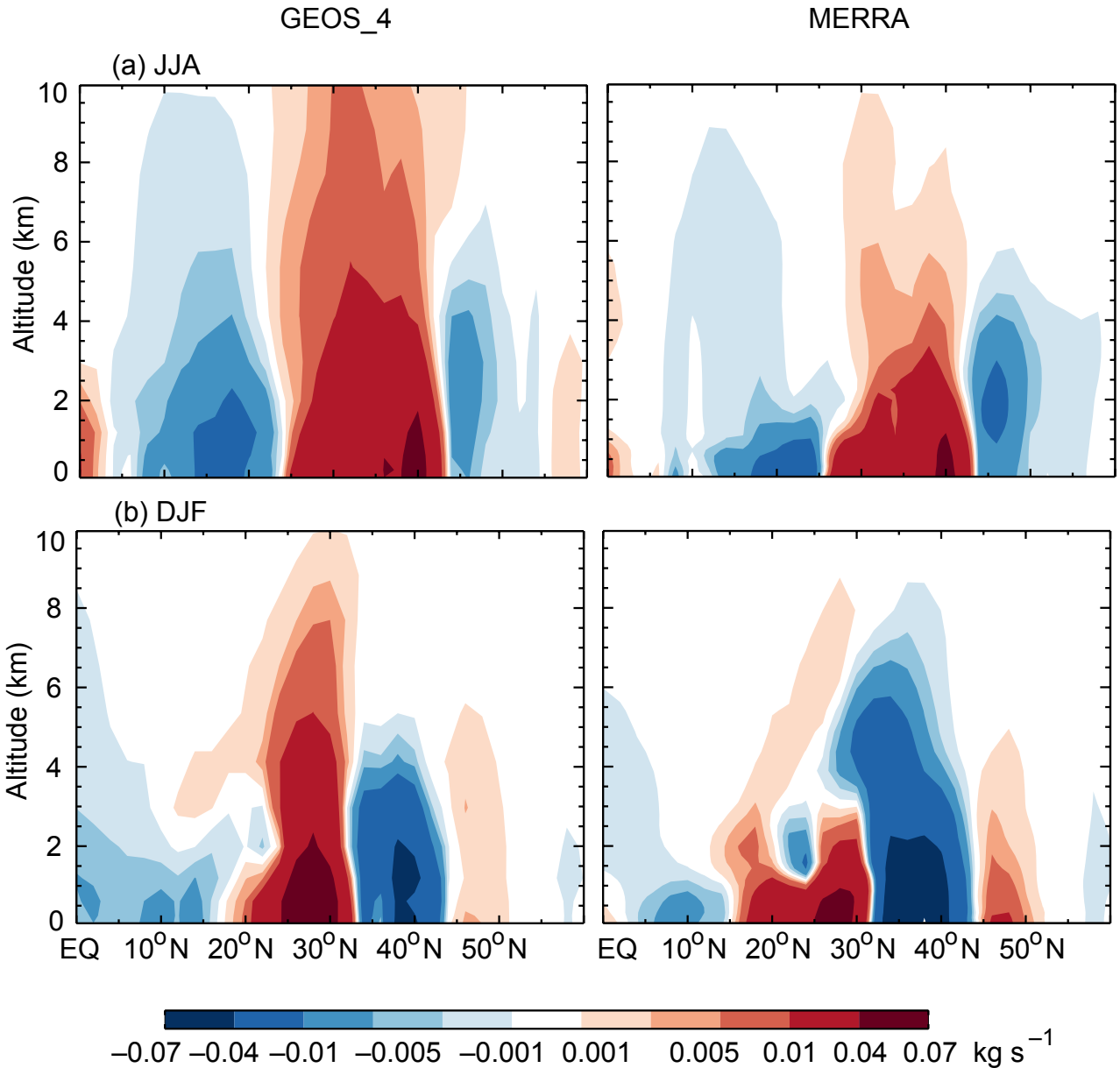


**Fig. 7. (a)** Differences in simulated upward mass flux of JJA BC (kg $s^{-1}$) between the five weakest and five strongest EASM years during 1986–2006. Plots are averaged over longitude range of 110–125° E from model simulations VMETG4 (left) and VMET (right). **(b)** Same as **(a)**, but for differences in DJF between five weakest and five strongest EAWM years.

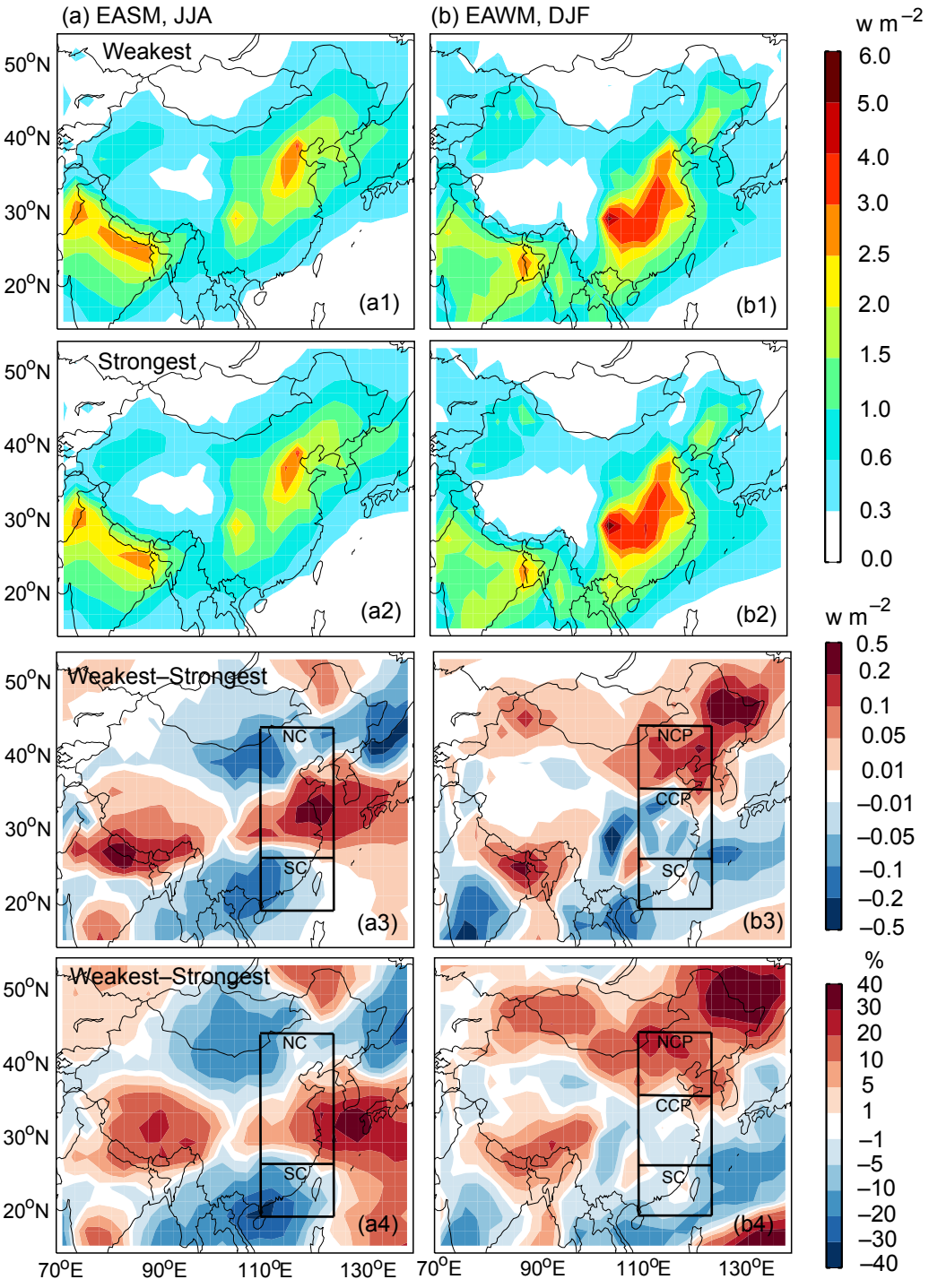


**Fig. 8. (a)** Simulated JJA mean all-sky direct radiative forcing (DRF) of BC (W $m^{-2}$) at the top of the atmosphere (TOA) in the **(a1)** five weakest and **(a2)** five strongest EASM years during 1986–2006 from model simulation VMET. Also shown are the **(a3)** absolute (W $m^{-2}$) and **(a4)** percentage (%) differences between the five weakest and five strongest EASM years. **(b)** Same as **(a)**, but for simulated DJF mean all-sky TOA DRF of BC in the five weakest and five strongest EAWM years. The enclosed areas are defined as northern China (NC, 110–125° E, 28–45° N), the northern China Plain (NCP, 110–125° E, 36–45° N), the central China Plain (CCP, 110–125° E, 28–36° N), and southern China (SC, 110–125° E, 20–27° N).

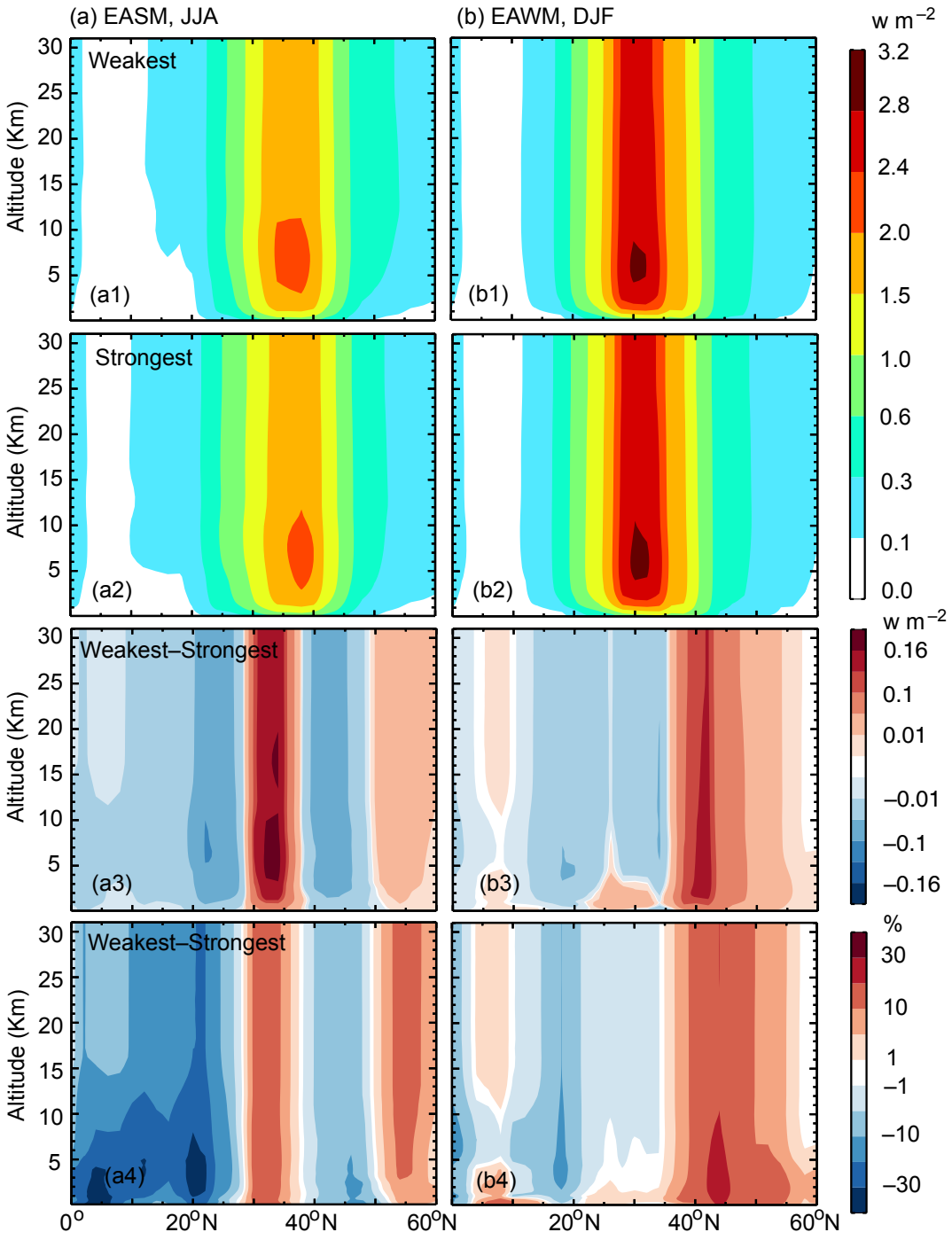


**Fig. 9. (a)** Height-latitude cross sections of simulated JJA mean all-sky DRF of BC (W m$^{-2}$) in the **(a1)** five weakest and **(a2)** five strongest EASM years during 1986–2006. Also shown are the **(a3)** absolute (W m$^{-2}$) and **(a4)** percentage (%) differences between the five weakest and five strongest EASM years. Plots are averaged over longitude range of 110–125° E from model simulation VMET. **(b)** Same as **(a)**, but for simulated DJF mean all-sky DRF of BC in the five weakest and five strongest EAWM years.

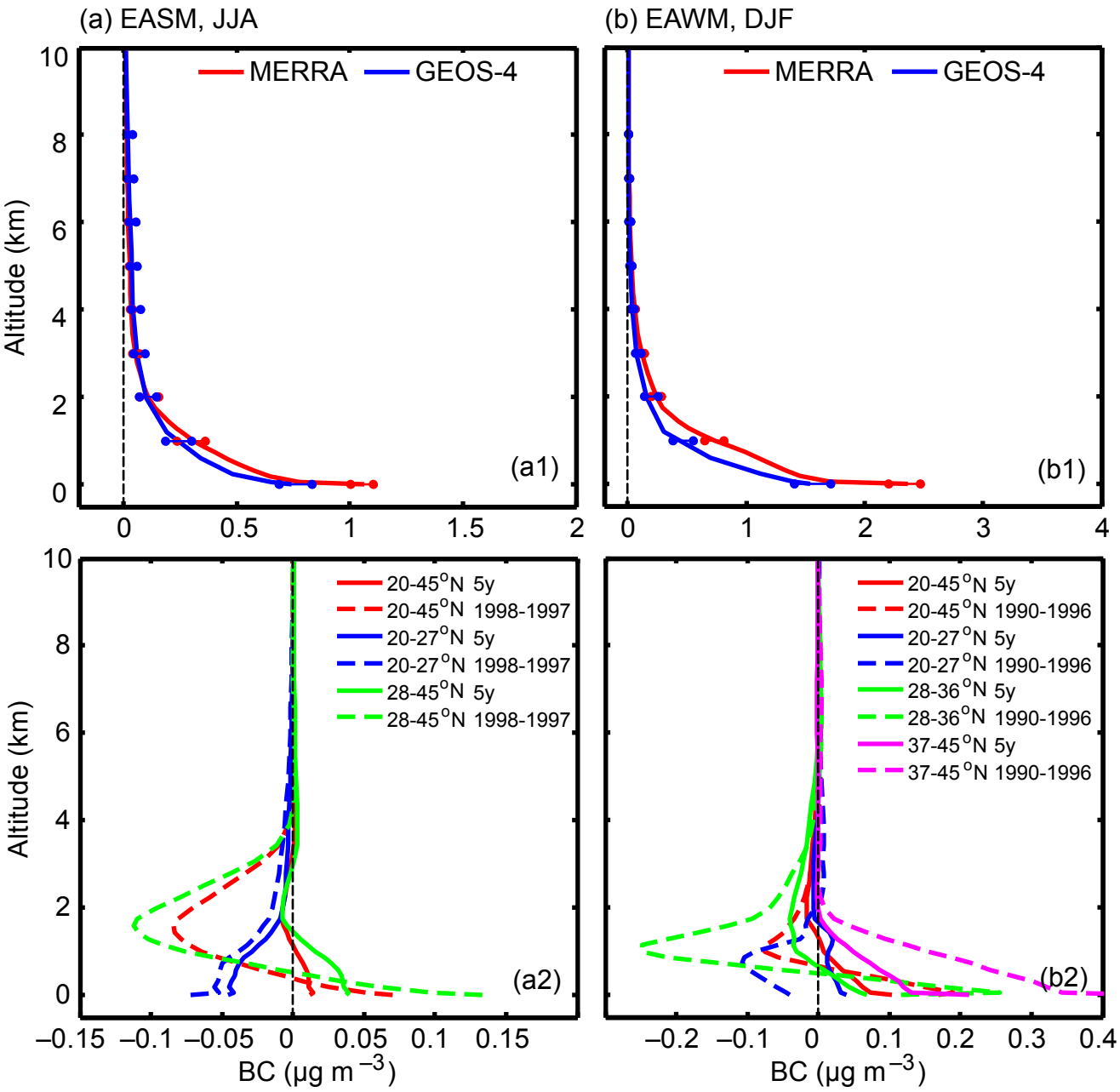


**Fig. 10. (a1)** Simulated vertical profiles of JJA BC mass concentrations (μg $m^{-3}$) averaged over 1986–2006. The error bars represent the minimum and maximum values of BC. Results are averages over eastern China from model simulations VMETG4 (blue) and VMET (red). **(a2)** Differences in simulated vertical profiles of JJA BC mass concentrations (μg $m^{-3}$) between the five weakest and five strongest EAM years (solid lines) during 1986–2006, and between the weakest and strongest EASM years (1998–1997, dotted lines)**.** Results are averages over eastern China, northern China, and southern China from model simulations VMET. **(b1)** Same as **(a1),** but for simulated DJF BC mass concentrations. **(b2)** Same as **(a2),** but for differences in DJF between the five weakest and five strongest EAWM years and between the weakest and strongest EAWM years (1990–1996). Results are averages over eastern China, northern China Plain, the central China Plain, and southern China.

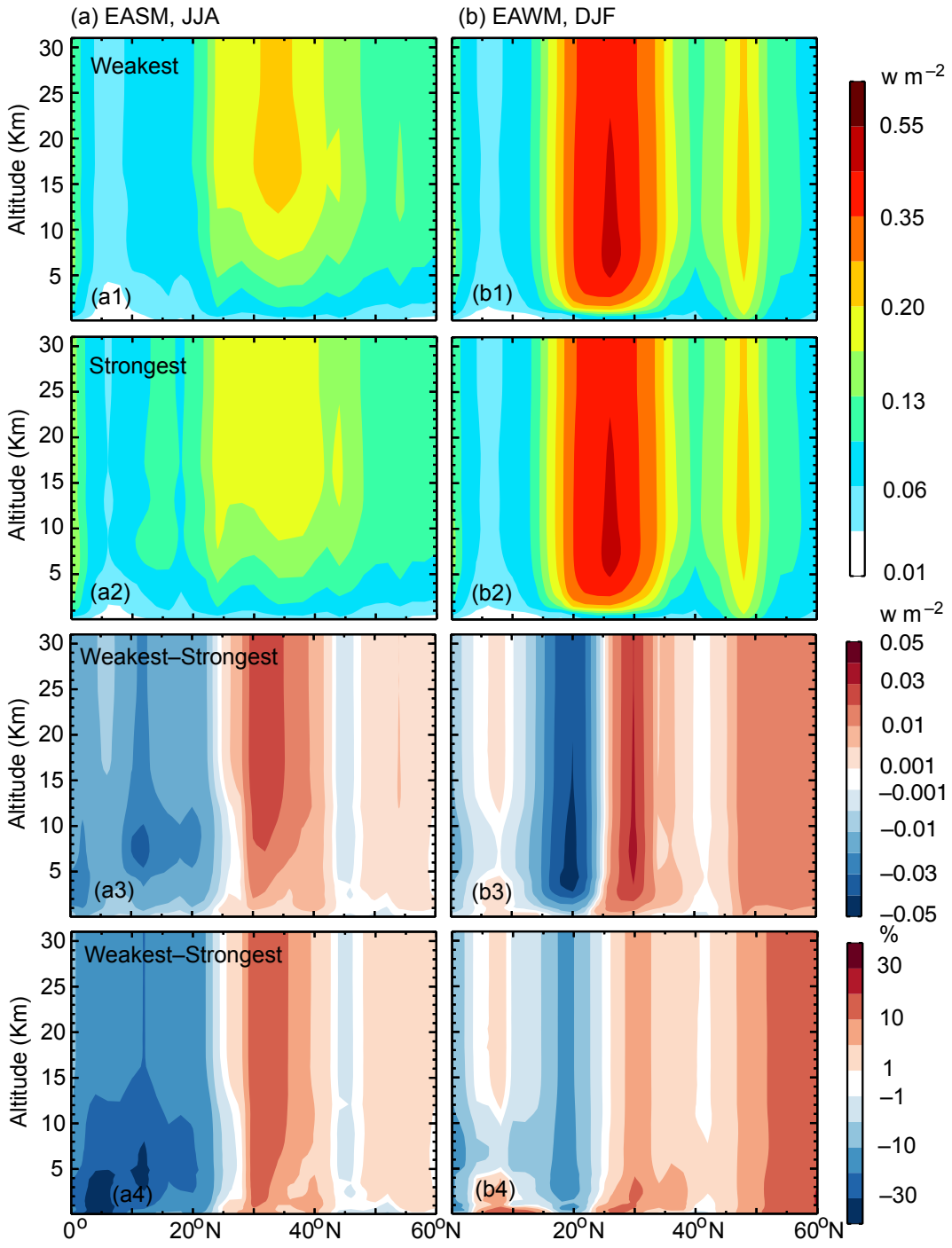


**Figure 11.** Same as **Figure 9,** but for the contributions from non-China emissions to simulated all sky DRF ~~of~~ of BC .

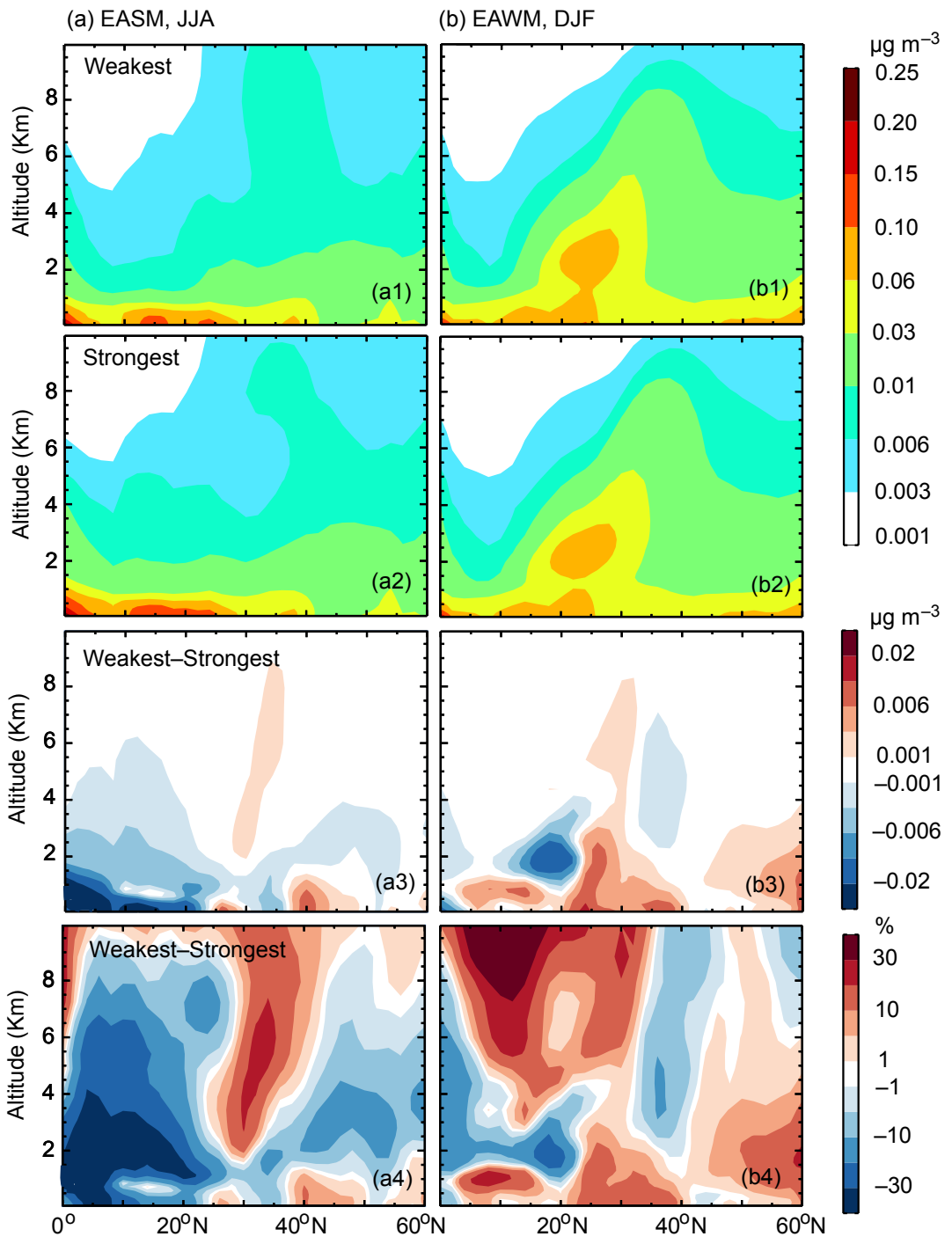


**Fig. 12. (a)** Height-latitude cross sections of contributions of non-China emissions to simulated JJA mean BC concentrations (μg $m^{-3}$) in the **(a1)** five weakest and **(a2)** five strongest EASM years during 1986–2006. Also shown are the **(a3)** absolute (μg $m^{-3}$) and **(a4)** percentage (%) differences between the five weakest and five strongest EASM years. Plots are averaged over longitude range of 110–125° E from model simulation VMET. **(b)** Same as **(a)**, but for simulated DJF mean BC concentrations in the five weakest and five strongest EAWM years.

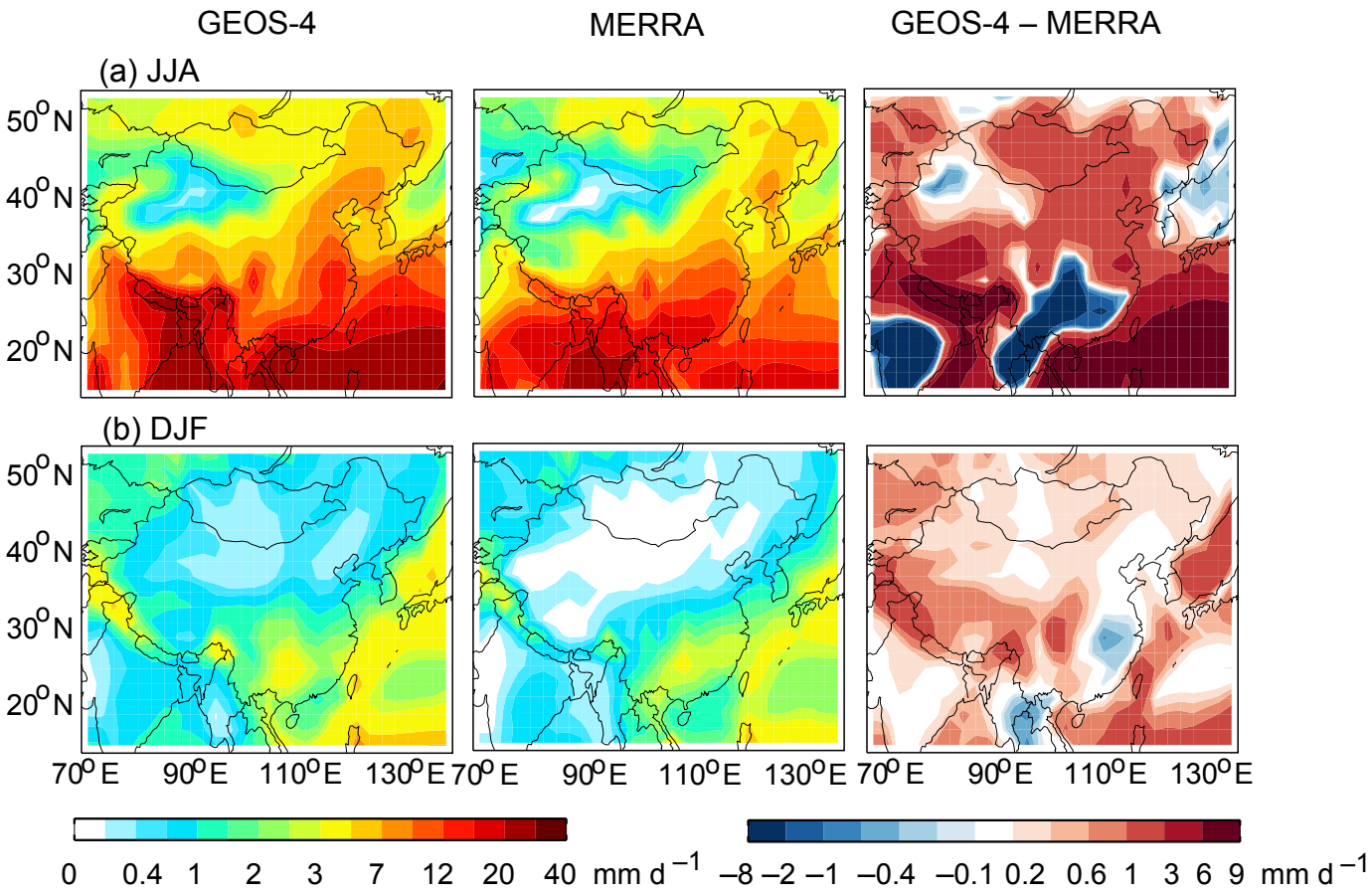


**Fig. 1S .** JJA and DJF mean precipitation (mm $d^{-1}$) averaged for 1986–2006 from GEOS-4 **(a)** and MERRA **(b)** meteorological data. Also shown are the differences between GEOS-4 and MERRA data **(c)**.

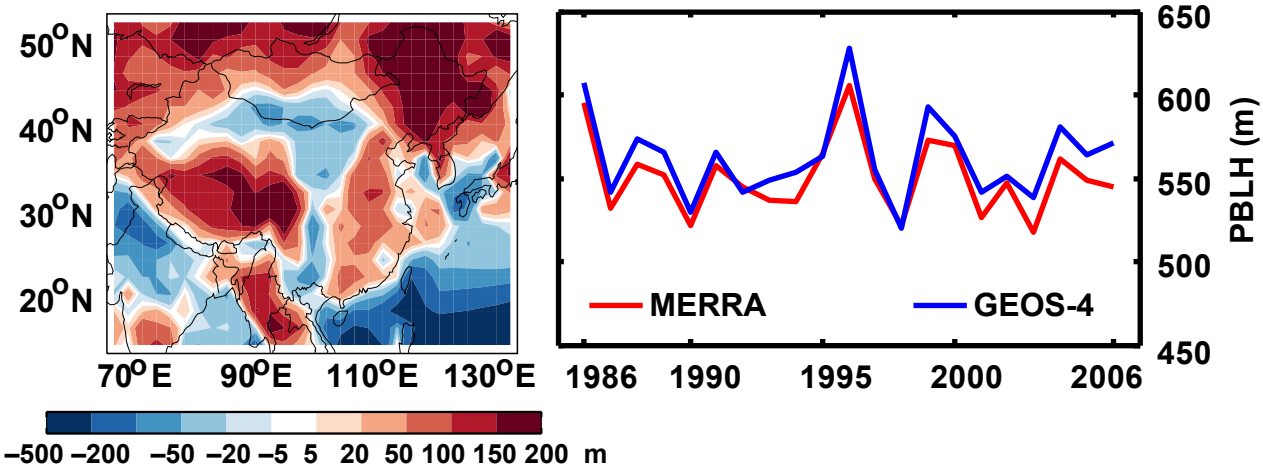


**Fig. 2S. (left)** Differences in DJF mean planetary boundary layer height (PBLH, m) averaged for 1986–2006 between GEOS-4 and MERRA. **(right)** DJF mean PBLH averaged over eastern China for 1986–2006 from GEOS-4 (blue line) and MERRA (red line).